

**SIMULINK-MODEL BASED STUDY OF  
FLOW RATE CHARACTERISTIC OF  
DIRECTIONAL CONTROL VALVE  
UNDER DIFFERENT FAULT  
CONDITIONS**

**M.Tech. Thesis**

By  
**ANSHUL CHAUDHARY**  
(2002103017)



**DEPARTMENT OF MECHANICAL ENGINEERING  
INDIAN INSTITUTE OF TECHNOLOGY  
INDORE**

**MAY 2022**



# **SIMULINK-MODEL BASED STUDY OF FLOW RATE CHARACTERISTIC OF DIRECTIONAL CONTROL VALVE UNDER DIFFERENT FAULT CONDITIONS**

**A THESIS**

*Submitted in partial fulfillment of the  
requirements for the award of the degree*

*of*

**Master of Technology**

*by*

**ANSHUL CHAUDHARY**



**DEPARTMENT OF MECHANICAL ENGINEERING  
INDIAN INSTITUTE OF TECHNOLOGY  
INDORE**

**MAY 2022**





# INDIAN INSTITUTE OF TECHNOLOGY INDORE

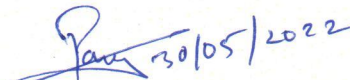
## CANDIDATE'S DECLARATION

I hereby certify that the work which is being presented in the thesis entitled **SIMULINK-MODEL BASED STUDY OF FLOW RATE CHARACTERISTIC OF DIRECTIONAL CONTROL VALVE UNDER DIFFERENT FAULT CONDITIONS** in the partial fulfillment of the requirements for the award of the degree of **MASTER OF TECHNOLOGY** and submitted in the **DEPARTMENT OF MECHANICAL ENGINEERING, Indian Institute of Technology Indore**, is an authentic record of my own work carried out during the time period from August 2020 to May 2022 under the supervision of **Dr. Pavan Kumar Kankar, Associate Professor, Department of Mechanical Engineering, Indian Institute of Technology** and **Dr. Ankur Miglani, Assistant Professor, Department of Mechanical Engineering, Indian Institute of Technology**.

The matter presented in this thesis has not been submitted by me for the award of any other degree of this or any other institute.

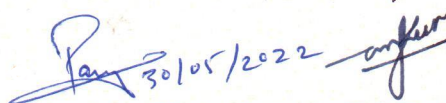
  
30/05/22  
(ANSHUL CHAUDHARY)

-----  
This is to certify that the above statement made by the candidate is correct to the best of our knowledge.

  
30/05/2022  
(Dr. PAVAN KUMAR KANKAR)

  
30 MAY 2022  
(Dr. ANKUR MIGLANI)

-----  
ANSHUL CHAUDHARY has successfully given his M.Tech. Oral Examination held on **May 24, 2022**.

  
Signature(s) of Supervisor(s) of M.Tech. thesis  
Date: 30 MAY 2022

  
Convener, DPGC  
Date: 30/05/22

  
Signature of PSPC Member #1  
(Dr. Ashish Rajak)  
Date: 31/5/2022

  
Signature of PSPC Member #2  
(Dr. Puneet Gupta)  
Date: 31-5-2022



## ACKNOWLEDGEMENT

My deep gratitude goes first to my supervisors, **Dr. Pavan Kumar Kankar** and **Dr. Ankur Miglani**, who expertly guided me throughout my two years of Master of Technology. I was fortunate to have advisors who offered me the constant motivation and productive support that preceded this work to attain this form. I would also like to thank my PSPC members, **Dr. Ashish Rajak** and **Dr. Puneet Gupta** for their continuous inputs for the advancement of this project.

My appreciation also extends to my laboratory colleagues. Mr. Jatin Prakash's (Ph.D. scholar) mentoring and encouragement have been especially valuable, and his early insights launched the greater part of this dissertation. Thanks to Mr. Vinod Singh Thakur (Ph.D scholar) and Mr. Nagendra Singh Ranawat (Ph.D scholar) who enriched my knowledge in the domain of condition monitoring. Thanks also goes to Mr. Sushil, Mr. Shrish, Mr. Rishabh, and my other batch-mates for their moral support throughout this journey.

I cannot end my words without expressing my heartfelt thanks and admiration for my dear parents' blessings and efforts to maintain my morale up throughout the duration of my project. I'd want to offer my heartfelt gratitude to everyone who has assisted me in any way, whether directly or indirectly, during this project.

With Regards,



Anshul Chaudhary



*Dedicated*  
*to*  
*My beloved*  
*Parents*



## **Abstract**

Directional control valves perform a vital role in operating any hydraulic system accurately. It is a component working continuously with the fluid flowing at high pressure and controlling the volume and direction of the fluid to be supplied to the actuator. Any component working under such circumstances is prone to failure. The failure in the DC valve can be in the form of leakage due to wear at the surface of any internal part. Also due to moisture inside the valve, corrosion and binding may result in improper movement of spool and can lead to spool stuck situation.

This project studies the flow rate behaviour of a four-port three-way directional control valve under ideal conditions and multiple leakage faults situations. The flow rate characteristic curve under healthy parameters is used to form a comparison study with flow rate characteristic curves obtained under leakage fault conditions. In the later part of the study, fault in spool movement is also incorporated, causing the improper opening of the orifice, and affecting the desired flow rate.

From the comparison study of leakage, it has been concluded that the variation of flow rate is less with 10% fault in directional control valves as compared to the extreme case of 90% fault. And with fault in spool movement, we have observed that flow rate value increases with wear in orifice and then starts to decline with increase in fault in the spool.



# TABLE OF CONTENTS

Acknowledgement	(v)
Abstract	(ix)
List of Figures	(xv)
List of Tables	(xxi)
Nomenclature	(xxv)
1. Introduction	(1)
1.1. Overview	(1)
1.2. Directional control valves	(1)
1.2.1. Classification	(2)
1.3. Four-way, three-position directional control valves	(3)
1.3.1. Valve positions	(3)
1.4. Significance of the study	(4)
1.5. Thesis organization	(6)
2. Literature Review	(7)
2.1. Overview	(7)
2.2. Hydraulic systems	(7)
2.3. Maintenance strategies	(8)
2.4. Condition monitoring	(9)
2.5. Faults in directional control valves	(12)
3. Methodology	(13)
3.1. Overview	(13)
3.2. A model-based approach for determination of leakage in 4/3 DC	(13)
3.2.1. Components used to design the SIMULINK model	(14)
3.2.2. Parameters used in base model to validate it with previous studies and by mathematical model	(18)
3.3. Simulink-model based study to observe leakage at port 'A' of directional control valve	(19)



3.4. Simulink-model based study to observe variation in flow rate with healthy orifice and faulty spool movement	(22)
3.5. Simulink-model based study to observe variation in flow rate with multiple faulty orifice and faulty spool movement	(24)
4. Result and Discussion	(31)
4.1. Overview	(31)
4.2. Flow rate characteristics of 4/3- way DC valve SIMULINK model	(31)
4.3. Flow rate characteristics of DC valve with leakage through orifice “A”	(33)
4.4. Flow rate characteristics of DC valve with healthy orifice and faulty spool movement	(37)
4.5. Flow rate characteristics with multiple faulty orifice and faulty spool movement	(40)
4.6. Comparison of all five faulty cases	(60)
5. Conclusion and future scope	(63)
5.1. Conclusion	(63)
5.2. Future scope	(64)
References	(65)



## LIST OF FIGURES

Fig. 1.1: Classification of DC valves based on principal characteristics

Fig. 1.2: Schematic of 4/3-way DC valve

Fig. 1.3: Block diagram of 4/3 DC valve

Fig. 1.4: Closed state valve position

Fig. 1.5: Valve position with flow from port P to A, B to T

Fig. 1.6: Valve position with flow from port P to B, A to T

Fig. 2.1: Schematic of a basic hydraulic system

Fig. 2.2: Classification of maintenance strategy

Fig. 3.1: Model to study flow characteristic of DC valve

Fig. 3.2: Control signal for operation of DC valve

Fig. 3.3: Movement of spool over orifice with respect to the control signal

Fig. 3.4: Schematic of SIMULINK model with orifice faults

Fig. 3.5: Control signal from signal builder for healthy and faulty DC valve

Fig. 3.6: Schematic of SIMULINK model with Spool movement faults

Fig. 3.7: Schematic of SIMULINK model with multiple faulty orifice and spool movement faults

Fig. 4.1: Flow rate characteristics of 4/3 DC valve

Fig. 4.2: Schematic representation of hydraulic actuator connected to a 4-way directional control

Fig. 4.3: Comparison of flow rate characteristics of DC valve under multiple orifice faults



Fig. 4.4: Plot representing flow rate values under different orifice faults at time  $t=2$  sec

Fig 4.5: Plot representing flow rate values under different orifice faults at time  $t=8$  sec

Fig 4.6: Comparison of flow rate characteristics of DC valve under multiple spool faults

Fig 4.7: Plot representing flow rate values under multiple spool faults at time  $t=2$  sec

Fig 4.8: Plot representing flow rate values under multiple spool faults at time  $t=8$  sec

Fig 4.9: Comparison of flow rate characteristics of DC valve under 10% increase in orifice area and multiple spool faults

Fig 4.10: Plot representing flow rate values under 10% orifice fault and faulty spool movement at time,  $t=2$  seconds

Fig 4.11: Plot representing flow rate values under 10% orifice fault and faulty spool movement at time,  $t=8$  seconds

Fig 4.12: Comparison of flow rate characteristics of DC valve under 25% increase in orifice area and multiple spool faults

Fig 4.13: Plot representing flow rate values under 25% orifice fault and faulty spool movement at time,  $t=2$  seconds

Fig 4.14: Plot representing flow rate values under 25% orifice fault and faulty spool movement at time,  $t=8$  seconds

Fig 4.15: Comparison of flow rate characteristics of DC valve under 50% increase in orifice area and multiple spool faults

Fig 4.16: Plot representing flow rate values under 50% orifice fault and faulty spool movement at time,  $t=2$  seconds



Fig 4.17: Plot representing flow rate values under 50% orifice fault and faulty spool movement at time,  $t=8$  seconds

Fig 4.18: Comparison of flow rate characteristics of DC valve under 75% increase in orifice area and multiple spool faults

Fig 4.19: Plot representing flow rate values under 75% orifice fault and faulty spool movement at time,  $t=2$  seconds

Fig 4.20: Plot representing flow rate values under 75% orifice fault and faulty spool movement at time,  $t=8$  seconds

Fig 4.21: Comparison of flow rate characteristics of DC valve under 90% increase in orifice area and multiple spool faults

Fig 4.22: Plot representing flow rate values under 90% orifice fault and faulty spool movement at time,  $t=2$  seconds

Fig 4.23: Plot representing flow rate values under 90% orifice fault and faulty spool movement at time,  $t=8$  seconds

Fig 4.24: 3-D plot comparing all 5 cases at time,  $t=2$  seconds

Fig 4.25: 3-D plot comparing all 5 cases at time,  $t=8$  seconds



## LIST OF TABLES

Table 3.1: Parameter of 4/3 way DC valve block

Table 3.2: Opening area vectors according to the leakage condition

Table 3.3: Opening vector and opening area vector according to fault conditions

Table 3.4: Opening vector and opening area vector according to fault conditions for case 1

Table 3.5: Opening vector and opening area vector according to fault conditions for case 2

Table 3.6: Opening vector and opening area vector according to fault conditions for case 3

Table 3.7: Opening vector and opening area vector according to fault conditions for case 4

Table 3.8: Opening vector and opening area vector according to fault conditions for case 5

Table 4.1: Flow rate values with different orifice conditions at time,  $t=2$  seconds

Table 4.2: Flow rate values with different orifice conditions at time,  $t=8$  seconds

Table 4.3: Flow rate values with different orifice conditions due to faulty spool movement at time,  $t=2$  seconds

Table 4.4: Flow rate values with different orifice conditions due to faulty spool movement at time,  $t=8$  seconds

Table 4.5: Flow rate values with 10% orifice fault and faulty spool movement at time,  $t=2$  seconds



Table 4.6: Flow rate values with 10% orifice fault and faulty spool movement at time,  $t=8$  seconds

Table 4.7: Flow rate values with 25% orifice fault and faulty spool movement at time,  $t=2$  seconds

Table 4.8: Flow rate values with 25% orifice fault and faulty spool movement at time,  $t=8$  seconds

Table 4.9: Flow rate values with 50% orifice fault and faulty spool movement at time,  $t=2$  seconds

Table 4.10: Flow rate values with 50% orifice fault and faulty spool movement at time,  $t=8$  seconds

Table 4.11: Flow rate values with 75% orifice fault and faulty spool movement at time,  $t=2$  seconds

Table 4.12: Flow rate values with 75% orifice fault and faulty spool movement at time,  $t=8$  seconds

Table 4.13: Flow rate values with 90% orifice fault and faulty spool movement at time,  $t=2$  seconds

Table 4.14: Flow rate values with 90% orifice fault and faulty spool movement at time,  $t=8$  seconds

Table 4.15: Table defining axis of the plots in fig 4.24 and 4.25

Table 4.16: Table defining region 1 of the plots in fig 4.24 and 4.25



## ACRONYMS

- DC- Directional control
- 4/3 way- Four port three position
- LPM- Liter per Minute
- Q- Flow rate through orifice
- $C_d$ - Flow discharge coefficient
- A- Orifice area
- $x_v$ - control member displacement
- $P_s$ - Pressure at supply port
- $P_1$ - Pressure in cylinder at 1<sup>st</sup> port
- $P_2$ - Pressure in cylinder at 2<sup>nd</sup> port
- $\rho$ - Density of fluid



# Chapter 1

## Introduction

### 1.1 Overview

Hydraulic valves are often employed in hydraulic control systems to precisely modulate and regulate the entire system. The valve offers the connection amongst the hydraulic power element, i.e., the pump, as well as the actuator (linear or rotary) acting as the hydraulic output device equipped in valve-controlled hydraulic circuits.

In these circuits, the directional control valve is the component that collects response from the machinist or another automated control supply and modifies the system output as needed. When working with high-power devices, such as those found in hydraulic control circuits, this feedback is utilized to offer a regulated output or to offer a safety function [1].

Directional valves are utilized to change the fluid flow to the place in a hydraulic power system where it will accomplish work at a specific moment. When a directional control valve is employed, it is used to drive a ram backward and forward in its cylinder. Selector valves, transfer valves, and control valves are various terminologies used to describe directional valves [2].

The hydraulic directional valve is a crucial component extensively applied in industry and aerospace wherever hydraulic transmission is used [3].

### 1.2 Directional control valves

Directional control valves, as the names indicate, are used to control the flow direction [4]. Within hydraulic circuits, directional control valves are employed as switching devices [1]. The vast majority of industrial directional control valves have a finite positioning capability. They do this by opening and closing flow pathways in specific valve

configurations to control where the oil goes. There are multiple ways of operating a DC valve, for instance by creating pressure difference on parallel surfaces of valve sections or may be positioned manually, mechanically, or electrically [2].

### 1.2.1 Classification

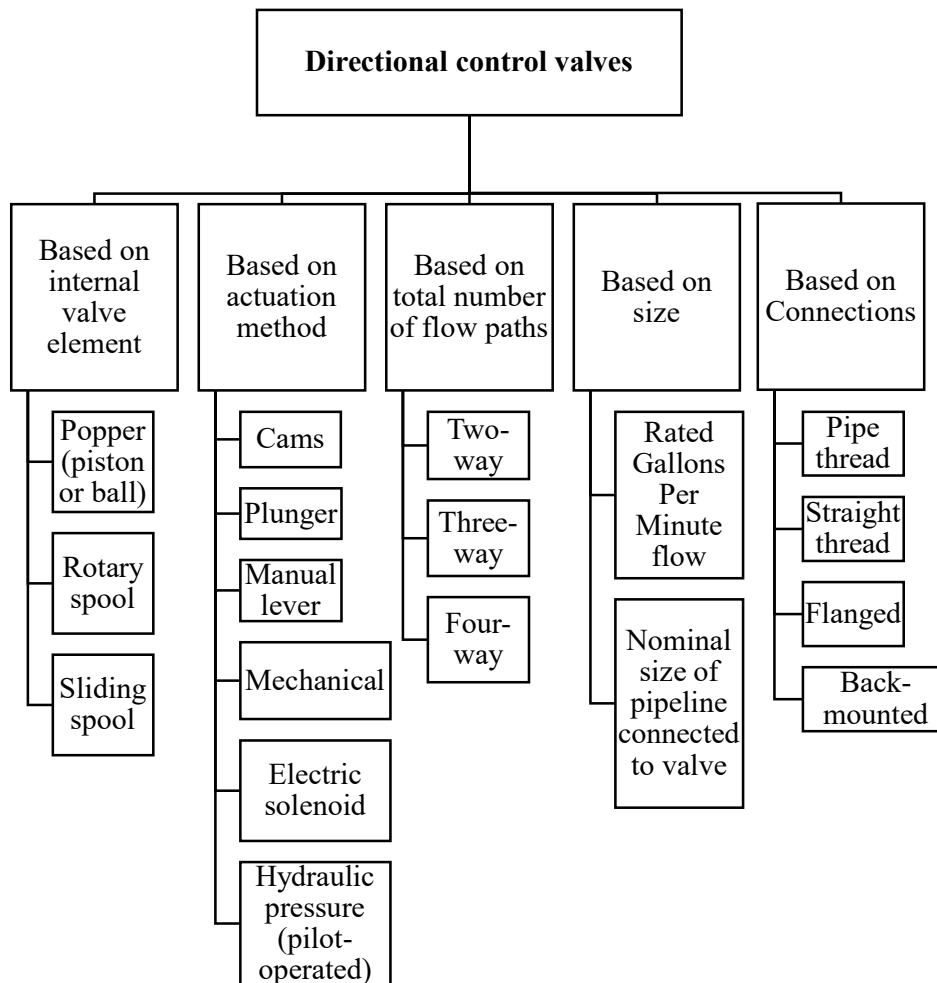


**Fig 1.1: Classification of DC valves based on principal characteristics**

The above flow chart lists directional control valves, classified based on internal valve elements, actuation method, total number of flow paths, size, and connections [4].

Mostly directional control valves are differentiated by the total number of flow paths in it, i.e., two-way, three-way, and four-way. This study is based on a 4-way 3-position or 4/3 DC valve which is discussed in detail in the next section.

### 1.3 Four-way, three-position directional control valve

A four-way, three-position DC valve has four ports to control fluid flow to the actuator. As shown in fig 1.2 below, port P is the supply port, and fluid enters the DC valve through it. Port 'A' and port 'B' are the ports connected to the actuator in the cylinder and are responsible for flowing fluid from the DC valve to it. Port T is the tank port that is used to direct the flow return to the tank. The same can also be observed in the block diagram of DC valve in fig 1.3.

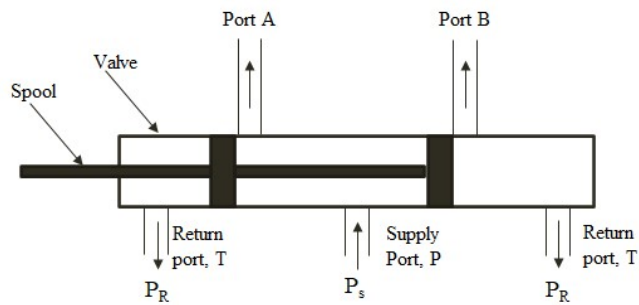


Fig 1.2: Schematic of 4/3-way DC valve

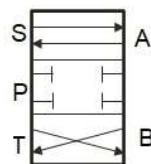
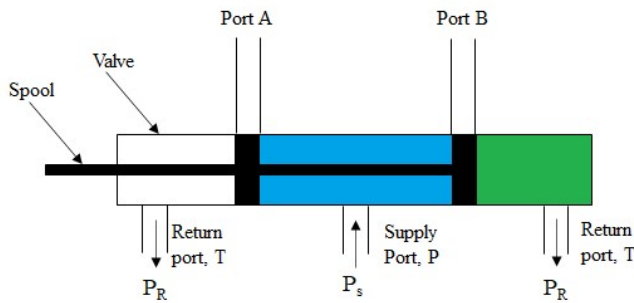


Fig 1.3: Block diagram of 4/3 DC valve

#### 1.3.1 Valve positions

The valve can be positioned in three ways. First case when the valve is in closed state. Secondly, when the fluid runs from port P to A and returns from port B to T. Third case is when fluid flows from port P to

B and returns from A to T. All three cases are depicted in fig 1.4, 1.5, 1.6 respectively.



**Fig 1.4: Closed state valve position**

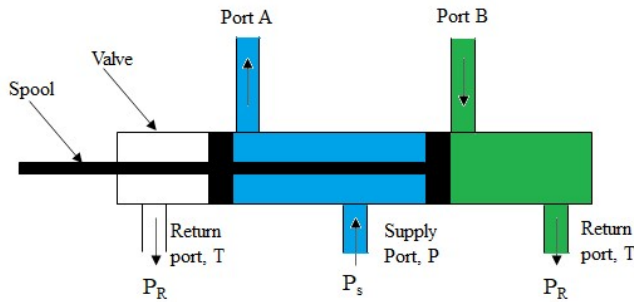


**Fig 1.5: Valve position with flow from port P to A, B to T**

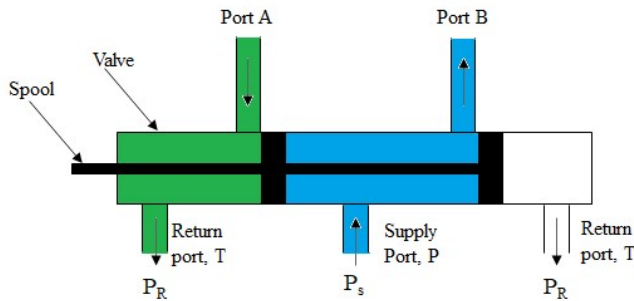


**Fig 1.6: Valve position with flow from port P to B, A to T**

### 1.4 Significance of the study

Leakage is an undesirable fault in any hydraulic system, but it is a challenging task to evade it from any component that operates with fluid entirely. Any hydraulic machine or its components tends to wear out due to fluid forces or fluid contamination and cause leakage[5]. This leakage may result in improper functioning of the component and complete

hydraulic system. This fault may lead to a complete breakdown of the system, accounting for a loss of time and resources. To prevent such incidents, condition monitoring techniques can be used to detect the fault in the system in advance.

Directional control valve has multiple orifices through which fluid enters and exits. These orifices may wear

out over a time of operation due to contamination in the fluid, causing an increase in its area. This wear will lead to leakage through it, causing an increase in the flow rate than desired.

Because of the faults being experienced in the DC valve component, this thesis proposes a SIMULINK model-based study to observe the variation in flow rate under multiple faulty conditions. The scope of the present analysis can be listed as follows:

- MATLAB-SIMULINK model of 4/3 DC valve and its parameters has been studied to observe its flow rate characteristics.
- After observing the flow rate under healthy conditions, leakage fault has been incorporated by varying different parameters of the DC valve block.
- The first case under this study is to observe the flow rate under leakage at a single port of a directional control valve by considering an increase in orifice area due to wear.
- The second case is a study of DC valve behaviour with faulty spool movement, causing the partial opening of the orifice and not delivering desired flow rate output.
- The third case is a study combining both the faults, i.e., multiple orifice faults with faulty spool movement.

## 1.5 Thesis organization

The thesis consists of five chapters. Each of them is described briefly in order to provide a clear understanding of the thesis's contents.

**Chapter 1** introduces hydraulic directional control valves and a brief about their classification. This chapter deals with explaining the four-way, three-position DC valve, and its functioning through valve positions. The aim and significance of the study have been highlighted in the end.

**Chapter 2** reviews the literature on the condition monitoring of directional control valves and hydraulic systems. It cites the novel contribution of the authors in the past to simulate the leakage fault in various hydraulic components and condition monitoring of them.

**Chapter 3** constitutes the methodology of a MATLAB-SIMULINK-based model study to observe the flow rate characteristics of a 4/3-way DC valve under a no-fault case, leakage through an orifice, faulty spool movement, and a combination of leakage and faulty spool movement.

**Chapter 4** explains the output of the cases discussed in chapter 3. In this chapter, a comparison study has been done by observing the changes in flow rate of DC valve under healthy and faulty conditions. Flow rate trends under multiple faulty conditions have been observed and plotted at different time intervals. These results are used to understand the physics behind the operation of the DC valve.

**Chapter 5** summarizes and concludes the research outcomes based on results obtained from multiple case studies. It also briefly discusses the future scope of the project.

# Chapter 2

## Literature review

### 2.1 Overview

This chapter covers a brief review of past research work in the field of condition monitoring of hydraulic systems and their components. A summary of maintenance strategies and condition monitoring techniques has been mentioned. Various methods, algorithms, and practices made by different academic and industry people have been discussed to meet more realistic approximations.

### 2.2 Hydraulic systems

Power transmission systems in which energy or signals are transmitted via static or dynamic forces of liquids are referred to as hydraulic systems [6]. These systems are broadly utilized in industrial applications of their characteristics like size-to-power ratio and capacity to apply tremendous forces and torques with quick reaction times[7] [8]. Industrial hydraulics remains comparatively new in the field of power transmission and control. Over the past five decades the manufacturing of modern industrial hydraulic components has increased very rapidly as it is an economical method to convert mechanical energy into fluid energy[9]. The range of control of force, speed and direction provided by fluid power transmission systems is unmatched with any other type of energy transmission. The growing trend of modern robots and computerised machinery being used in factories is made feasible in part by persistent improvement in this field[10].

A hydraulic system mainly comprises of components like cylinder (actuator), direction control valve, pump, motor, pressure regulator and fluid for system reservoir [11] as shown in fig

2.1, and hydraulics is defined as a method of transmitting power by pushing on a confined liquid, with the input component of the system as a pump and output as an actuator [4].

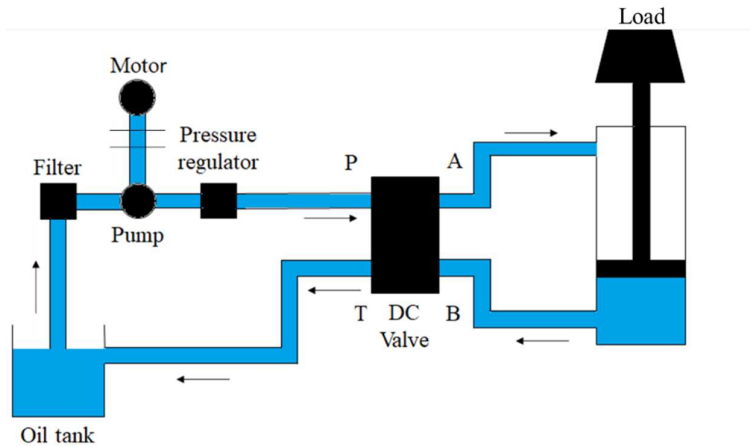


**Fig 2.1: Schematic of a basic hydraulic system**

Hydraulic systems have numerous applications, including electro-hydraulic positioning systems, material testing, active suspension control, hydraulic braking systems and industrial hydraulic systems. Reliability, safety, and economical detection of faults in the hydraulic system being monitored are some of the major concerns for these applications. Hydraulic systems involve a lot of complexity, and it operates under tough working conditions which makes the fault detection and diagnosis in such systems laborious. For better operational safety and economy of the system early detection of any fault in the component is important, making condition monitoring of the hydraulic system a very important technique in this field[12] [6].

## **2.3 Maintenance strategies**

Maintenance strategies can be classified into three categories [13]:

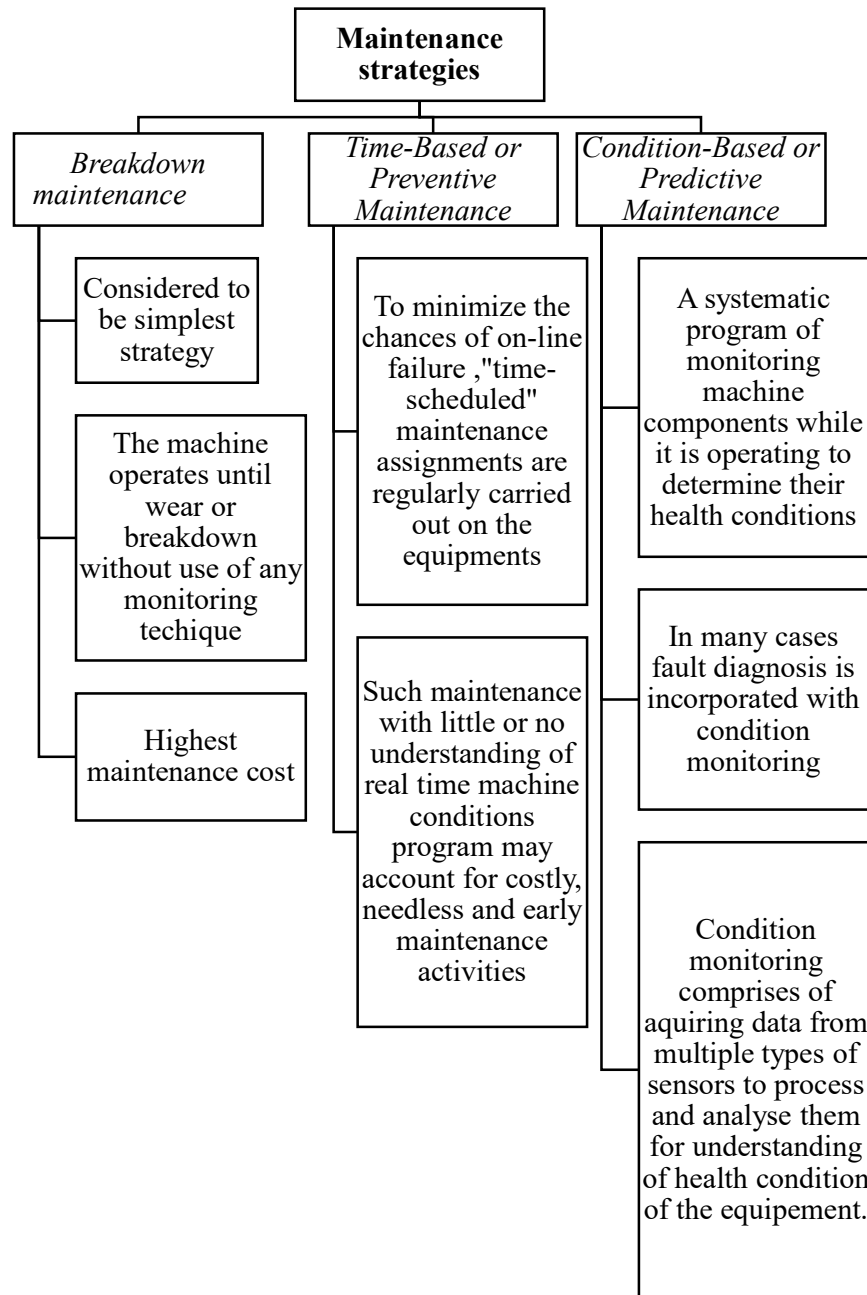


**Fig 2.2: Classification of maintenance strategy**

## **2.4 Condition monitoring**

Condition monitoring is a management technique that involves regular evaluations of the actual working condition of the plant's equipment,

production systems, and plant management activities to improve the plant operation [14].

System monitoring and diagnosis is a support technique which is used to increase the safety as well as expand the serviceability of any machine or component. In various applications, plants operate close to their design limit for a long period of time due to heightened requirements on production and performance. This may often lead to faults or failures in the system, which are commonly described by ongoing or crucial variations in the parameters of the system, or at the same time by variations in the system's intrinsic dynamics. Faults lead to gradual deprivation of the system's performance and if not corrected in due course, may account to failures resulting in loss of productivity and equipment, and be dangerous for human safety. Tighter safety and reliability measures have been imposed to incorporate safety from the effects of failures, which has resulted in more research in maintenance procedures[12].

Nowadays fluid power hardware is utilized in almost every business and are classified into two key different areas. First area involves high-level risk and elevated capital cost with application like nuclear energy, aerospace technology, and marine engineering. Even catastrophic being at a low level when assessed with the task, the causing loss of life is intolerable. In such conditions, failure in the beginning is restricted to arise by allowing the extra expenditure of early replacement. Most such malfunctions are accounted for only after they happen by depending on component's redundancy via a failure/safe operation.

The second area where fluid systems are often utilized comprises of applications like transportation engineering, mining, forestry, construction activity, material handling and machine tool equipment. This area is currently the most neglected from a monitoring perspective. In areas such as mining, fluid losses because of inessential part replacement, leakage in pipelines and hydraulic system components, etc., accounts in replacement costs or cost owing to occurring

catastrophes or inefficient operations. According to an estimation when a hydraulic system crashes, roughly sixty percent of the downtime is utilized in problem diagnosis, while the remaining 40 percent is utilized to repair or correct the fault [10].

To decrease the time and effort required in diagnosing the fault, numerous computerised tools have been developed and executed, which mainly practice knowledge-based skilled systems built on precise models of system's components and data from sensors [15][16][17].

In automated fault diagnosis using expert systems a major drawback arises in correctly including on-line sensor measurements. The information captured via sensor convey valuable data regarding the condition of the system are often varying with time, related to noise, non-robust and non-descriptive.

It has been a challenging work to turn these numeric data into comparative measures and rendering them in comprehensible linguistic terminology [18].

Adopting an advanced maintenance techniques which can monitor the working condition of a hydraulic machine, has many of the following benefits:

- Extended operating life
- Lower downtime as well as unscheduled maintenance
- Prevention from superfluous and early replacement of parts
- Non-stop and complete evaluation of intricate equipment in the system
- Improved protection and dependability
- Improved energy efficiency
- Identification of faulty working circumstances and part assemblies

Generally, two condition monitoring philosophies are used in hydraulic systems. First is the model-based approach, that requires comprehensive

physical and mathematical knowledge about the characteristics of the system, and second is the statistical approach, which is based on analysis of previously studied faults and measurement data associated with it and requires appropriate amounts of historical data [19].

## **2.5 Faults in directional control valves**

Control valves are mechanical components that experience wear and tear over time. They may build up a large dead band, increased static friction or stiction, saturation, backlash, corrosion on valve seat, wear in diaphragm, and other issues with time [20]. Various other common faults are discussed briefly below [21]:

- Valve clogging: It is caused by dust particles aggregating at the valve's inlet, developing in erroneous output flow characteristics.
- Positioner supply pressure drop: This issue happens when there is a clog or leakage in the supply pipeline, resulting in limited supply pressure to the diaphragm, impacting the stem movement.
- Fully or partially opened bypass valve: This is due to inaccurate inflow caused by a flow valve fault in the bypass path, causing faulty outflow.
- Fault in flow rate sensor: Even if the outflow is correct, the controller may make erroneous modifications as a result of the incorrect flow rate measurement.
- Internal leakage: It occurs as a consequence of erosion all around the valve seat and can result in a liquid flow even when the valve is closed [22] [23] [24].
- Stem displacement fault: It happens due to physical misalignment in the stem and can lead to erroneous transmission of diaphragm to the shutting and opening of a valve.

In this thesis, the study is focused on two faults, i.e., leakage through an orifice and faulty spool movement.

## Chapter 3

# Methodology

### 3.1 Overview

MATLAB-SIMULINK based model study has been carried out to observe the flow rate characteristics of a 4/3-way DC valve under

- Healthy case, i.e., no fault is there in the component
- Leakage through an orifice
- Faulty movement of spool, causing undesired orifice openings
- Combination of leakage and faulty spool movement

A base model to study the healthy condition of DC valve is created in SIMULINK and the further faulty conditions are observed by varying the parameters of the 4/3-way directional control valves.

### 3.2 A model-based approach for determination of leakage in 4/3 DC

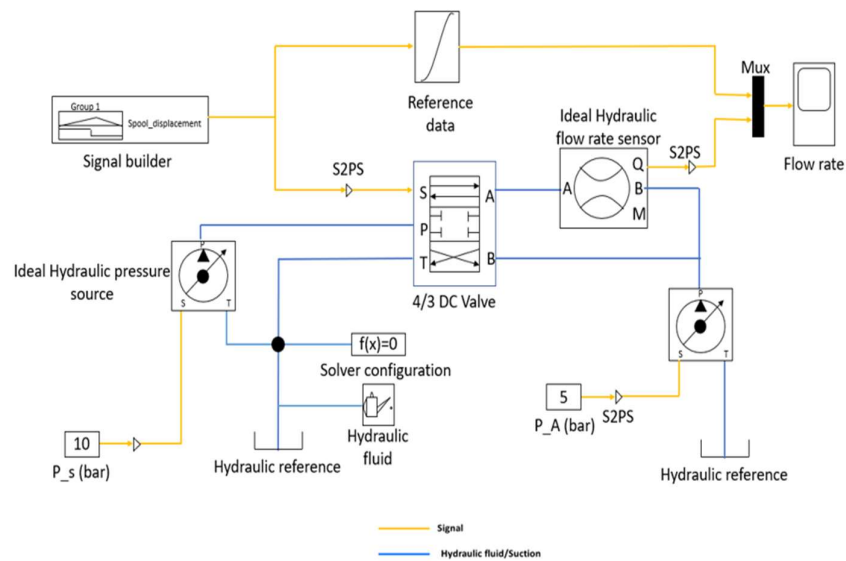


**Fig 3.1: Model to study flow characteristic of DC valve**

The above figure (3.1) shows the schematic of SIMULINK model for a directional control valve [25]. The DC valve block is connected to

control devices that operates it, like signal builder and hydraulic pressure source. The flow rate from port A is measured by using ideal hydraulic flow rate sensor and observed in scope block. These all components are discussed in detail in the next section of this chapter.

### **3.2.1 Components used to design the SIMULINK model[26]**

#### **1. 4/3-DC valve**

This block models the basic option of the 4-way directional valve in a hydraulic network. To parameterize the block, 3 options are available: (1) maximum area and control member stroke, (2) the table of valve area vs. control member displacement, and (3) the pressure- flow rate characteristics.

Ports:

- S- Control member displacement  
It is a port that inputs physical signal for control member displacement.
- P- Supply pressure connection port  
It is a port that relates with the inlet of pressure resource line.
- T- Port connected to tank or return line
- A and B- Ports connected to actuator  
These are ports that are correlated with the connection to the actuator.

Table 3.1: Parameter of 4/3 way DC valve block

<b>Fundamental Parameters</b>	
Area characteristics	<ul style="list-style-type: none"> <li>i. Identical for all flow paths</li> <li>ii. Different for each flow path</li> </ul>
Model parameterization	<ul style="list-style-type: none"> <li>i. Maximum area and opening</li> <li>ii. Area v/s opening table</li> <li>iii. Pressure-flow characteristics</li> </ul>
Leakage area	$A_{\text{leak}} (\text{m}^2) = 1\text{e-}12 \text{ m}^2$
Flow discharge coefficient	0.7
Laminar transition specification	Pressure ratio
Laminar flow pressure ratio	0.999

- Area characteristics

This parameter provides us with a variety of different or same flow path opening properties. Different flow path can be selected to give flow path parameters or formulated data individually for each flow path.

- Simulink-Model parameterization

- i. Maximum area and opening: This is the default parameter in DC valve block that indicate the full orifice opening and opening area. It changes linearly with respect to the spool movement stipulated at physical signal port S.
- ii. Area v/s opening table: This parameterization specifies the streamline opening area at distinct orifice opening. The orifice open region is calculated by interpolation or extrapolation of the listed data.

- iii. Pressure-flow characteristic: This parameterization is used to postulate volumetric flow rates of the flow path at distinct orifice openings as well as pressure differentials.

- Leakage area

This parameter defines the complete area of internal leaks between valve inlet in absolutely closed state of DC valve. It has a default value of  $1e-12 \text{ m}^2$ . The reason behind using this constraint is to retain the numerical integrity of the fluid system by inhibiting a part of that link from turning out to be isolated when the valve is in absolutely closed state.

- Flow discharge coefficient

It is a semi-empirical variable for valve capacity characterization with a default value of 0.7. Flow discharge coefficient is the ratio of the real and theoretical flow rates through the valve which is dependent on the geometrical characteristics of the valve.

- Laminar transition specification

This parameter defines the laminar-turbulent transition, which can be done by pressure ratio or Reynold's number.

Pressure ratio: Flow conversions from laminar to turbulent occurs at a predefined value in the laminar flow pressure ratio, i.e., 0.999. This option provides the user with the easiest and most numerically robust flow transition.

Reynold's number- Flow transition occurs at the Reynold's number predefined in the critical Reynold's number parameter, i.e., 12.

## **2. Signal builder**

The Signal Builder block is used to create control signals that are fed to the blocks in the model to operate them in a certain way as required by the user.

## **3. Ideal hydraulic flow rate sensor**

The Hydraulic Flow Rate Sensor block is a volumetric flow metre, or a tool that translates volumetric flow rate via hydraulic line into a proportional control signal. The volumetric flow rate value is output by connection Q, which is a physical signal port. The mass flow rate value is output from connection M, which is a physical signal port.

As it does not account for inertia, friction, delays, pressure loss, and other relevant factors, the sensor is ideal.

Hydraulic ports attaching the sensor to the hydraulic line are A and B. The positive direction of the sensor is from A to B.

## **4. Ideal hydraulic pressure source**

The Hydraulic Pressure Source component characterizes an ideal supply of hydraulic energy, capable of maintaining a defined pressure at its outlet independent of the flow rate.

The hydraulic inlet and outlet ports are denoted by block links T and P, respectively, and the control signal port is represented by block connection S.

To obtain the necessary pressure variation profile, you can utilise any of the Simulink® signal sources.

The positive orientation of the block is from port P to port T.

### 3.2.2 Parameters used in base model to validate it with previous studies and by mathematical model [25][27]

#### 1. 4/3-way DC valve

The basic parameters used are same as shown in table 3.1.

The flow rates are monitored with a pressure drop of 5 bar on each metering line in the exterior valve loop (P-A-B-T).

Ideal hydraulic pressure is required to maintain a pressure drop of 5 bar across all orifices.

The pressures at the P, A, and B ports are adjusted to 10 bar, 5 bar, and 5 bar, respectively, using source blocks.

#### 2. Signal builder

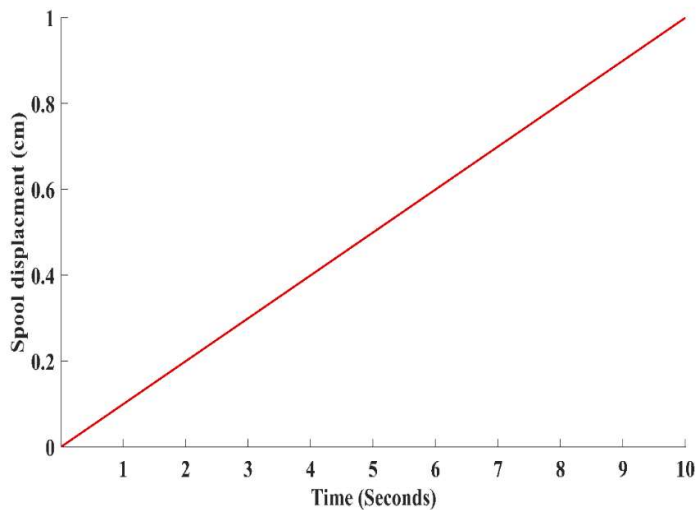


**Fig 3.2: Control signal for operation of DC valve**

The control signal in fig (3.2) shows the spool displacement (cm) v/s time (sec) which is generated in the signal builder and input in the DC valve control member displacement port (S).

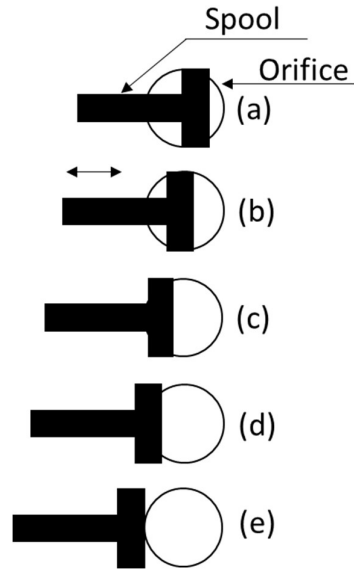


**Fig 3.3: Movement of spool over orifice with respect to the control signal**

The figure (3.3) shown above describes the motion of spool over orifice of directional control valves when the signal builder feeds signal to it.

The fig (3.3) a shows 20% spool movement over a period of 2 seconds.

The fig (3.3) b shows 40% spool movement over a period of 4 seconds.

The fig (3.3) c shows 60% spool movement over a period of 6 seconds.

The fig (3.3) d shows 80% spool movement over a period of 8 seconds.

The fig (3.3) e shows 100% spool movement over a period of 10 seconds

### **3.3 Simulink-model based study to observe leakage at port 'A' of directional control valve**

The model as shown in the figure (3.1) is used to study the flow rate characteristic of DC valve under multiple faulty orifice conditions.

Models with faulty orifice such as to create an increase in orifice area by 10%, 25%, 50%, 75% and 90% are connected and the flow rate characteristic output of each model is compared to the flow rate characteristic of the DC valve with healthy orifice.

The 4/3 DC valve block in the model is parameterized by using area v/s opening table parameters. The default values of it are considered for the healthy model having P to A, opening vector as [-.002, 0.0, 0.002, 0.005, 0.015] m and P-A, opening area vector as [1e-9, 2.0352e-7, 4.0736e-5, 0.00011438, 0.00034356] m<sup>2</sup> [26] . Now, the opening area vector is increased according to the fault condition required to be modelled. For example, to add a leakage fault of 10%, the opening area vector is increased by 10% ([1.1e-09, 2.055552e-07, 4.114336e-05, 1.155238e-04, 3.469956e-04]) keeping the opening vector same. The table below summarizes opening vector of all the cases,

Table 3.2: Opening area vectors according to the leakage condition

<b>Leakage percentage</b>	<b>Opening area vector</b>
0 (Healthy case)	[1e-09, 2.0352e-07, 4.0736e-05, 0.00011438, 0.00034356]
10	[1.1e-09, 2.055552e-07, 4.114336e-05, 1.155238e-04, 3.469956e-04]
25	[1.25e-09, 2.544e-07, 5.092e-05, 1.392975e-04, 4.2945e-04]
50	[1.5e-09, 3.0528e-07, 6.1104e-05, 1.7157e-04, 5.1534e-04]
75	[1.75e-09, 3.5616e-07, 7.1288e-05, 2.00165e-04, 6.0123e-04]
90	[1.9e-09, 3.86688e-07, 7.73984e-05, 2.17322e-04, 6.52764e-04]

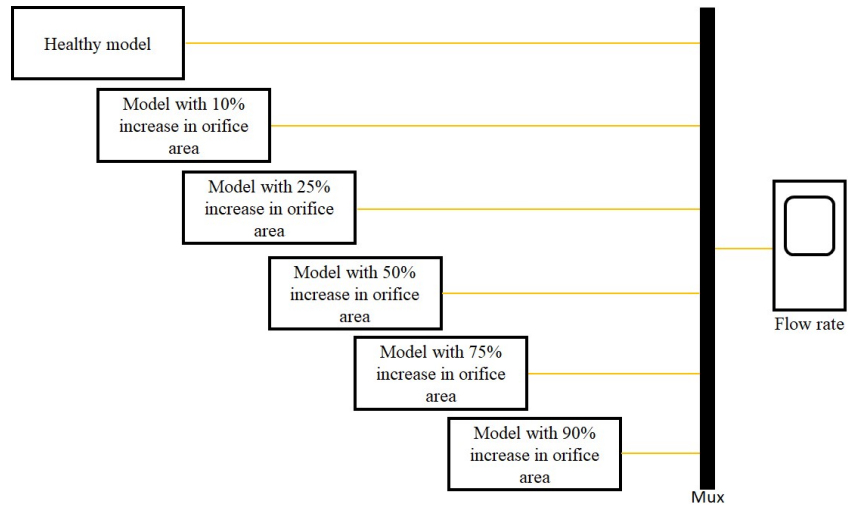


**Fig 3.4: Schematic of SIMULINK model with orifice faults**

The above figure depicts the schematic arrangement of healthy and faulty directional control valves model in SIMULINK to observe the comparison of flow rate in healthy and leakage conditions.

To operate the DC valve in each model in fig (3.4), signal builder inputs the same signal as show below:

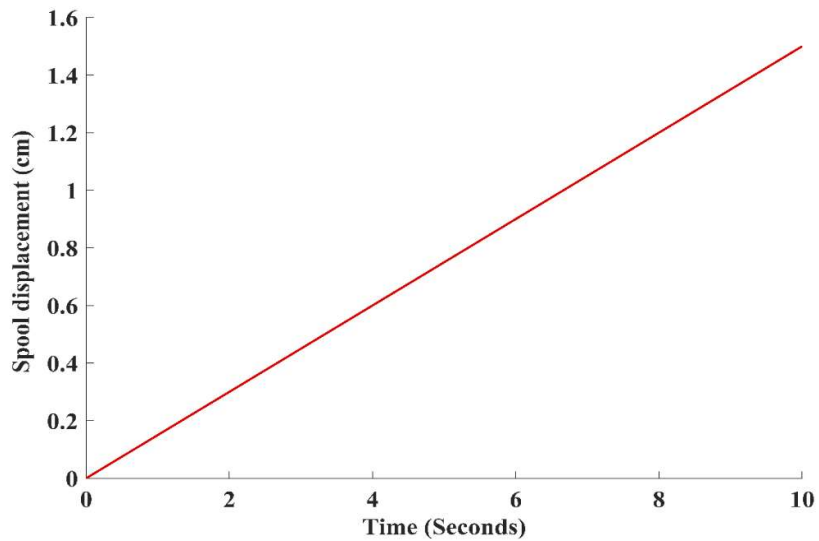


**Fig 3.5: Control signal from signal builder for healthy and faulty DC valve**

### 3.4 Simulink-model based study to observe variation in flow rate with healthy orifice and faulty spool movement

The base model as shown in the fig (3.1) is used to study the flow rate characteristic of dc valve under a condition where spool stuck in between its movement and does not create the desired orifice opening. Models with faulty spool such as to create an orifice opening of 90%, 75%, 50%, 25% and 10%, i.e., accounting to a fault of 10%, 25%, 50%, 75% and 90% respectively, are connected to a model with healthy spool causing no fault in orifice opening. The flow rate characteristic output of each model is compared to the flow rate characteristic of the DC valve with healthy spool.

The 4/3 DC valve block in the model is parameterized by using area v/s opening table parameters. The default values of it are considered for the healthy model having P to A, opening vector as [-0.002, 0.0, 0.002, 0.005, 0.015] m and P-A, opening area vector as [1.e-9, 2.0352e-7, 4.0736e-5, 0.00011438, 0.00034356] m<sup>2</sup> [26]. Now, the P-A opening vector is increased according to the fault condition required to be modelled and the required changes are made in opening area vector according to the values of opening vector. For example, to add a fault of 10%, the opening vector is increased by 10% ([-.0022, 0, .0022, .0055, .0165]) and the opening area vector is decreased by 10% ([0.9e-09, 1.83168e-07, 3.66624e-05, 1.02942e-04, 3.09204e-04]). The table below summarizes parameters of all the cases,

Table 3.3: Opening vector and opening area vector according to fault conditions

Model	Opening vector	Opening area vector
Healthy	[-.002, 0.0, 0.002, 0.005, 0.015]	[1.e-9, 2.0352e-7, 4.0736e-5, 0.00011438, 0.00034356]
90% orifice opening	[-.0022, 0, .0022, .0055, .0165]	[0.9e-09, 1.83168e-07, 3.66624e-05, 1.02942e-04, 3.09204e-04]

75% orifice opening	[-.0025, 0, .0025, .00625, .01875]	[0.75e-09, 1.5264e-07, 3.0552e-05, 8.5785e-05, 2.5767e-04]
50% orifice opening	[-.003, 0, .003, .0075, .0225]	[0.5e-09, 1.0176e-07, 2.0368e-05, 5.719e-05, 1.7178e-04]
25% orifice opening	[-.0035, 0, .0035, .00875, .02625]	[0.25e-09, 0.5088e-07, 1.0184e-05, 2.8595e-05, 8.589e-05]
10% orifice opening	[-.0038, 0, .0038, .0095, .0285]	[0.1e-09, .20352e-07, .40736e-05, .000011438, .000034356]

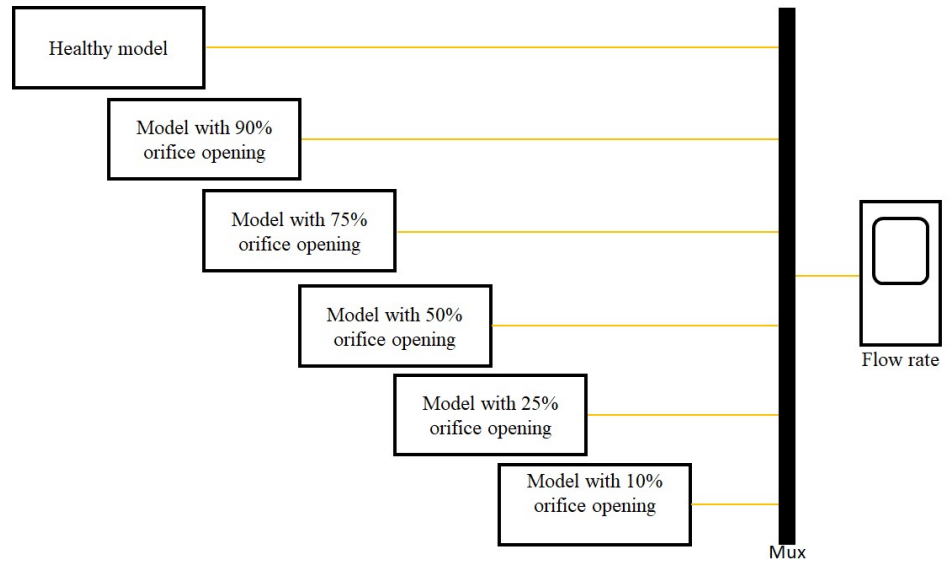


**Fig 3.6: Schematic of SIMULINK model with Spool movement faults**

The above figure depicts the schematic arrangement of healthy and faulty models in SIMULINK to observe the comparison of flow rate in all conditions.

To operate the DC valve in each model, signal builder inputs the same signal as show in fig (3.5).

### 3.5 Simulink-model based study to observe variation in flow rate with multiple faulty orifice and faulty spool movement

The base model as shown in the fig (3.1) is used to study the flow rate characteristic of dc valve under a condition where the orifice wears out and its opening area increases, and spool stuck in between its movement and does not allow the desired flow rate. Models with faulty spool such as to create an orifice opening of 90%, 75%, 50%, 25% and 10% over a wear out orifice causing an increase in opening area of 10%, 25%, 50%, 75% and 90%, i.e., accounting to a fault of 10%, 25%, 50%, 75% and 90% respectively, are connected to a healthy model. The flow rate characteristic output of each model is compared to the flow rate characteristic of the healthy DC valve.

#### Case 1: 10% orifice fault

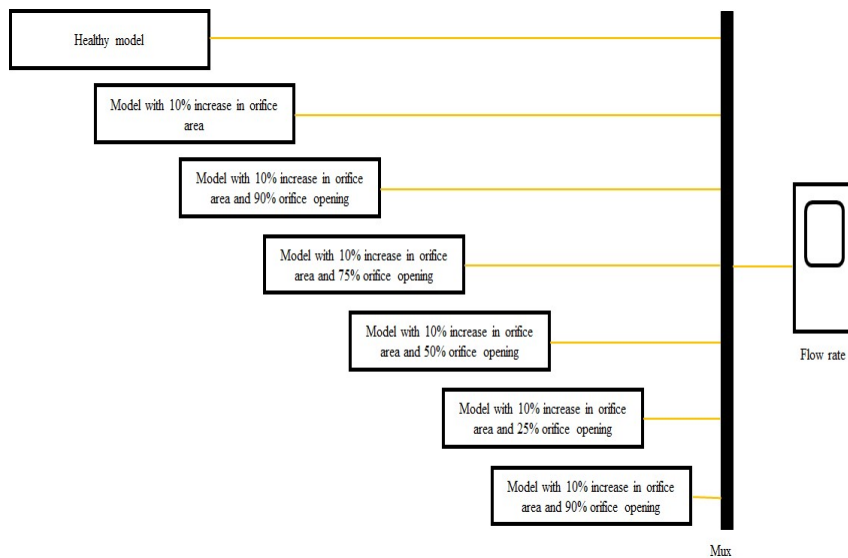


**Fig 3.7: Schematic of SIMULINK model with multiple faulty orifice and spool movement faults**

The above figure depicts the schematic arrangement of healthy and faulty models in SIMULINK to observe the comparison of flow rate in all conditions.

To operate the DC valve in each model signal builder inputs the same signal as show in fig (3.5).

The 4/3 DC valve block in the model is parameterized by using area v/s opening table parameters. The default values of it are considered for the healthy model having P to A, opening vector as [-0.002, 0.0, 0.002, 0.005, 0.015] m and P-A, opening area vector as [1e-9, 2.0352e-7, 4.0736e-5, 0.00011438, 0.00034356] m<sup>2</sup> [26]. For the model with 10% increase in orifice area, the P-A opening area vector is increased by 10% ([1.1e-09, 2.055552e-07, 4.114336e-05, 1.155238e-04, 3.469956e-04]). Now, the P-A opening vector is increased according to the fault condition required in spool position to be modelled. For example, in the model with 10% increase in orifice area and 90% orifice opening, the opening vector is increased by 10% ([-.0022, 0, .0022, .0055, .0165]) and orifice opening vector is decreased by 10% ([0.99e-09, 2.014848e-07, 4.032864e-05, 1.132362e-04, 3.401244e-04]) in the parameters of the DC valve block of model with 10% increase in orifice area. The table below summarizes parameters of all the cases,

Table 3.4: Opening vector and opening area vector according to fault conditions for case 1

<b>Model</b>	<b>Opening vector</b>	<b>Opening area vector</b>
Healthy	[-.002, 0, .002, .005, .015]	[1e-9, 2.0352e-7, 4.0736e-5, 0.00011438, 0.00034356]
10% increase in orifice area	[-.002, 0, .002, .005, .015]	[1.1e-09, 2.055552e-07, 4.114336e-05, 1.155238e-04, 3.469956e-04]
10% increase in orifice area and 90% orifice opening	[-.0022, 0, .0022, .0055, .0165]	[0.99e-09, 2.014848e-07, 4.032864e-05, 1.132362e-04, 3.401244e-04]
10% increase in orifice area and 75% orifice opening	[-.0025, 0, .0025, .00625, .01875]	[0.825e-09, 1.67904e-07, 3.36072e-05, 9.43635e-05, 2.83437e-04]

10% increase in orifice area and 50% orifice opening	[-.003, 0, .003, .0075, .0225]	[0.55e-09, 1.11936e-07, 2.24048e-05, 6.2909e-05, 1.88958e-04]
10% increase in orifice area and 25% orifice opening	[-.0035, 0, .0035, .00875, .02625]	[0.275e-09, 0.55968e-07, 1.12024e-05, 3.14545e-05, 9.4479e-05]
10% increase in orifice area and 10% orifice opening	[-.0038, 0, .0038, .0095, .0285]	[.11e-09, .223872e-07, .448096e-05, 1.25818e-05, 3.77916e-05]

By using the same methodology, multiple cases are studied and the variation in flow rate characteristics are observed. The cases are described below,

### Case 2: 25% orifice fault

Table 3.5: Opening vector and opening area vector according to fault conditions for case 2

Model	Opening vector	Opening area vector
Healthy	[-.002, 0, .002, .005, .015]	[1e-9, 2.0352e-7, 4.0736e-5, 0.00011438, 0.00034356]
25% increase in orifice area	[-.002, 0, .002, .005, .015]	[1.25e-09, 2.544e-07, 5.092e-05, 1.392975e-04, 4.2945e-04]
25% increase in orifice area and 90% orifice opening	[-.0022, 0, .0022, .0055, .0165]	[1.125e-09, 2.2896e-07, 4.5828e-05, 1.2536775e-04, 3.86505e-04]
25% increase in orifice area and 75% orifice opening	[-.0025, 0, .0025, .00625, .01875]	[0.9375e-09, 1.908e-07, 3.819e-05, 1.04473125e-04, 3.220875e-04]

25% increase in orifice area and 50% orifice opening	[-.003, 0, .003, .0075, .0225]	[0.625e-09, 1.272e-07, 2.546e-05, 0.6964875e-04, 2.14725e-04]
25% increase in orifice area and 25% orifice opening	[-.0035, 0, .0035, .00875, .02625]	[0.3125e-09, 0.636e-07, 1.273e-05, 0.348243e-04, 1.073625e-04]
25% increase in orifice area and 10% orifice opening	[-.0038, 0, .0038, .0095, .0285]	[.125e-09, .2544e-07, .5092e-05, .1392975e-04, .42945e-04]

### Case 3: 50% orifice fault

Table 3.6: Opening vector and opening area vector according to fault conditions for case 3

Model	Opening vector	Opening area vector
Healthy	[-.002, 0, .002, .005, .015]	[1e-9, 2.0352e-7, 4.0736e-5, 0.00011438, 0.00034356]
50% increase in orifice area	[-.002, 0, .002, .005, .015]	[1.5e-09, 3.0528e-07, 6.1104e-05, 1.7157e-04, 5.1534e-04]
50% increase in orifice area and 90% orifice opening	[-.0022, 0, .0022, .0055, .0165]	[1.35e-09, 2.74752e-07, 5.49936e-05, 1.54413e-04, 4.63806e-04]
50% increase in orifice area and 75% orifice opening	[-.0025, 0, .0025, .00625, .01875]	[1.125e-09, 2.2896e-07, 4.5828e-05, 1.286775e-04, 3.86505e-04]
50% increase in orifice area and 50% orifice opening	[-.003, 0, .003, .0075, .0225]	[0.75e-09, 1.5264e-07, 3.0552e-05, 0.85785e-04, 2.5767e-04]

50% increase in orifice area and 25% orifice opening	[-.0035, 0, .0035, .00875, .02625]	[0.375e-09, 0.7632e-07, 1.5276e-05, 0.428925e-04, 1.28835e-04]
50% increase in orifice area and 10% orifice opening	[-.0038, 0, .0038, .0095, .0285]	[.15e-09, .30528e-07, .61104e-05, .17157e-04, .51534e-04]

**Case 4: 75% orifice fault**

Table 3.7: Opening vector and opening area vector according to fault conditions for case 4

<b>Model</b>	<b>Opening vector</b>	<b>Opening area vector</b>
Healthy	[-.002, 0, .002, .005, .015]	[1e-9, 2.0352e-7, 4.0736e-5, 0.00011438, 0.00034356]
75% increase in orifice area	[-.002, 0, .002, .005, .015]	[1.75e-09, 3.5616e-07, 7.1288e-05, 2.00165e-04, 6.0123e-04]
75% increase in orifice area and 90% orifice opening	[-.0022, 0, .0022, .0055, .0165]	[1.575e-09, 3.20544e-07, 6.41592e-05, 1.801485e-04, 5.41107e-04]
75% increase in orifice area and 75% orifice opening	[-.0025, 0, .0025, .00625, .01875]	[1.3125e-09, 2.6712e-07, 5.3466e-05, 1.5012375e-04, 4.509225e-04]
75% increase in orifice area and 50% orifice opening	[-.003, 0, .003, .0075, .0225]	[0.875e-09, 1.7808e-07, 3.5644e-05, 1.000825e-04, 3.00615e-04]
75% increase in orifice area and 25% orifice opening	[-.0035, 0, .0035, .00875, .02625]	[0.4375e-09, 0.8904e-07, 1.7822e-05, 0.5004125e-04, 1.503075e-04]

75% increase in orifice area and 10% orifice opening	[-.0038, 0, .0038, .0095, .0285]	[.175e-09, .35616e-07, .71288e-05, .200165e-04, .60123e-04]
--	----------------------------------	---

### Case 5: 90% orifice fault

Table 3.8: Opening vector and opening area vector according to fault conditions for case 5

Model	Opening vector	Opening area vector
Healthy	[-.002, 0, .002, .005, .015]	[1e-9, 2.0352e-7, 4.0736e-5, 0.00011438, 0.00034356]
90% increase in orifice area	[-.002, 0, .002, .005, .015]	[1.9e-09, 3.86688e-07, 7.73984e-05, 2.17322e-04, 6.52764e-04]
90% increase in orifice area and 90% orifice opening	[-.0022, 0, .0022, .0055, .0165]	[1.71e-09, 3.480192e-07, 6.965856e-05, 1.955898e-04, 5.874876e-04]
90% increase in orifice area and 75% orifice opening	[-.0025, 0, .0025, .00625, .01875]	[1.425e-09, 2.90016e-07, 5.80488e-05, 1.629915e-04, 4.89573e-04]
90% increase in orifice area and 50% orifice opening	[-.003, 0, .003, .0075, .0225]	[0.95e-09, 1.93344e-07, 3.86992e-05, 1.08661e-04, 3.26382e-04]
90% increase in orifice area and 25% orifice opening	[-.0035, 0, .0035, .00875, .02625]	[0.475e-09, 0.96672e-07, 1.93496e-05, 0.543305e-04, 1.63191e-04]
90% increase in orifice area and 10% orifice opening	[-.0038, 0, .0038, .0095, .0285]	[.19e-09, .386688e-07, .773984e-05, .217322e-04, .652764e-04]



## **Chapter 4**

### **Result and Discussion**

#### **4.1 Overview**

In this chapter the flow rate characteristic of each model studied in chapter 3 are discussed and explained.

First the output of base model as shown in figure (3.1) is discussed and compared with the reference data in the model, along with the flow rate mathematical expressions. After studying the base model, the output of model considering leakage at an orifice is discussed and the flow rate comparison plot obtained is analyzed at different time intervals. Furthermore, the discussion is extended to observe the flow rate characteristics with faulty spool movement over a healthy orifice and flow rate characteristics with faulty spool movement and multiple orifice fault.

#### **4.2 Flow rate characteristics of 4/3- way DC valve**

##### **SIMULINK model**

The SIMULINK model of 4/3 DC valve as shown in fig (3.1) is run at the mentioned parameters in methodology section 3.2.2.1 and flow rate characteristics of it are observed in comparison to the reference data.

Reference data

Input signal- 0:0.1:1; (cm)

Flow rate- [0 0 52 150 248 346 450 540 625 670 700]; (l/min)

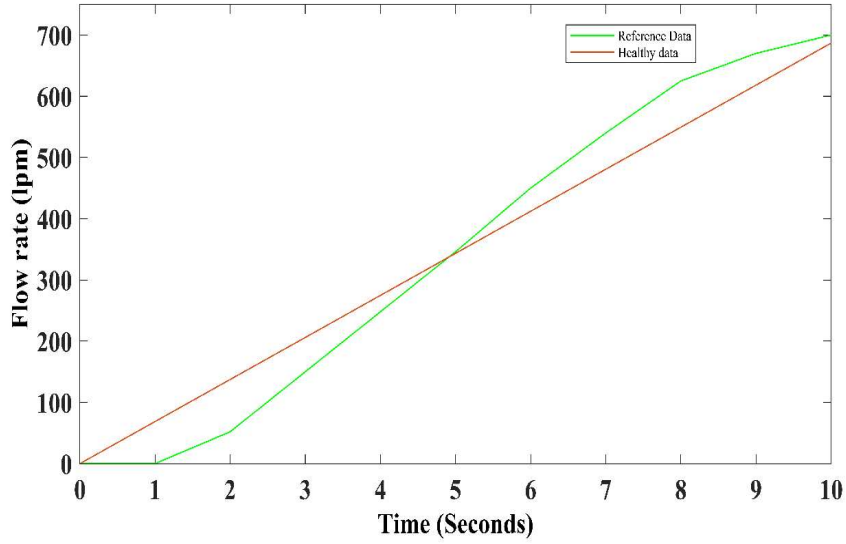


**Fig 4.1: Flow rate characteristics of 4/3 DC valve**

The above characteristics plot shows an increasing flow rate trend with respect to time as the opening of orifice increases. The same can be seen by the mathematical expressions of flow rate[27],

$$Q_1 = C_d A x_v s (P_s - P_1) \sqrt{\frac{2}{\rho} |P_s - P_1|} , x_v > 0. \quad (1)$$

$$Q_1 = C_d A x_v \frac{2}{\rho} P_1 , x_v < 0. \quad (2)$$

$$Q_2 = - C_d A x_v s (P_s - P_2) \sqrt{\frac{2}{\rho} |P_s - P_2|} , x_v < 0. \quad (3)$$

$$Q_2 = C_d A x_v \frac{2}{\rho} P_2 , x_v > 0. \quad (4)$$

Where,

Q- Flow rate through orifice

C<sub>d</sub>- Flow discharge coefficient

A- Orifice area

x<sub>v</sub>- control member displacement

P<sub>s</sub>- Pressure at supply port

P<sub>1</sub>- Pressure in cylinder at 1<sup>st</sup> port

$P_2$ - Pressure in cylinder at 2<sup>nd</sup> port

$\rho$ - Density of fluid

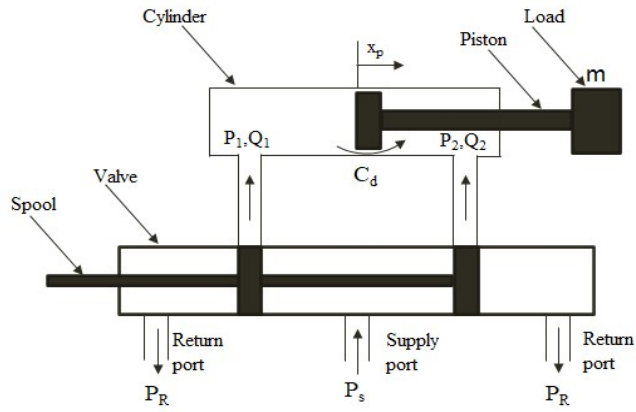


**Fig 4.2: Schematic representation of hydraulic actuator connected to a 4-way directional control valve**

### 4.3 Flow rate characteristics of DC valve with leakage through orifice “A”

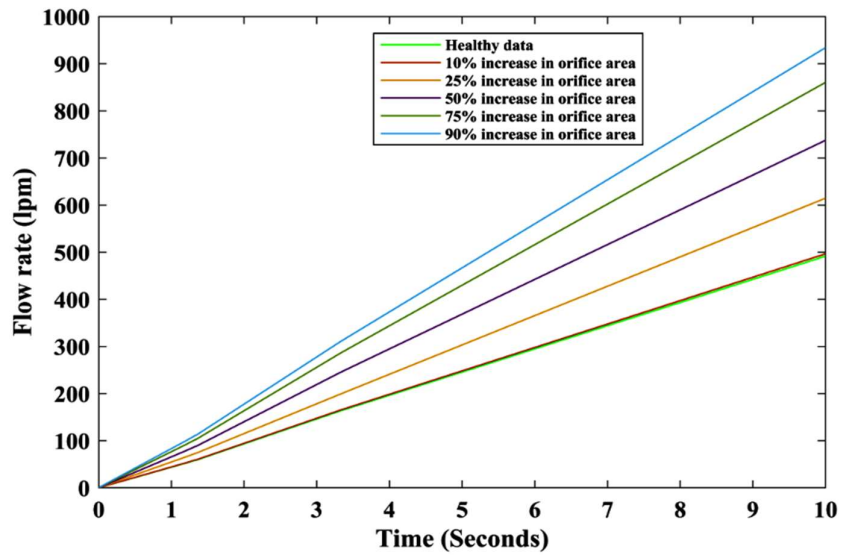


**Fig 4.3: Comparison of flow rate characteristics of DC valve under multiple orifice faults**

The graph in figure (4.3) above shows a comparison of flow rate output from each model connected in a combination as shown in schematic figure (3.4). We can observe that as the area of the orifice is increasing due to wear, the flow rate tends to increase along with it. The variation is least in the case of 10% orifice fault and max in case of 90% orifice fault.

To understand the change in flow rate characteristics of each model, the below tables show the comparison of flow rate values at time, t=2 seconds and t=8 seconds.

Table 4.1: Flow rate values with different orifice conditions at time, t=2 seconds

<b>Model</b>	<b>Flow rate (lpm) at, t = 2 seconds</b>	<b>Difference compared to healthy data</b>
Healthy	93.4	-
10% increase in orifice area	94.3	0.9
25% increase in orifice area	115	21.6
50% increase in orifice area	140	46.6
75% increase in orifice area	163	69.6
90% increase in orifice area	177	83.6

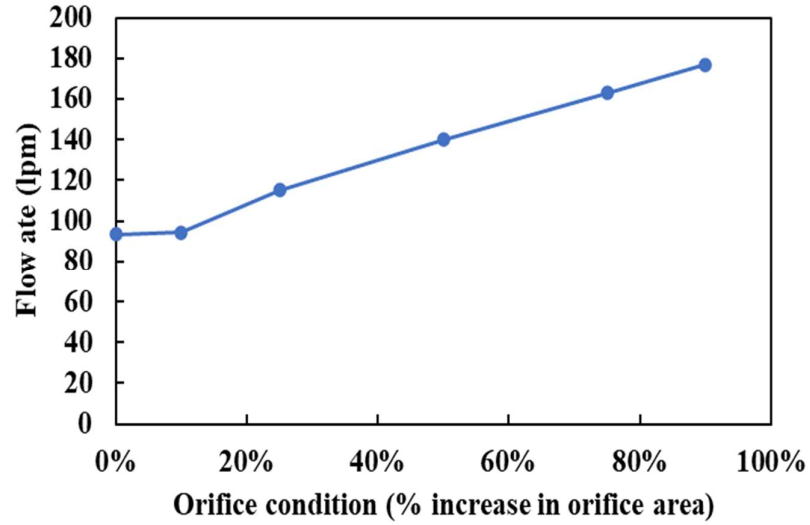


**Fig 4.4: Plot representing flow rate values under different orifice faults at time  $t=2$  sec.**

From table 4.1 and plot in fig 4.4, we can observe that the leakage at 10% fault is less as compared to the leakage when the DC valve is run at 90% fault. The same can be observed from the curves in graph (fig 4.3), which shows the flow rate characteristic of 10% increase in orifice area, almost overlapping with the healthy case, whereas there is observable increase in flow rate in other cases. It can also be observed that the cumulative difference increases up to 50% fault and then slightly decreases, i.e., variation is more in beginning of the fault and then gradually reduces.

**Table 4.2: Flow rate values with different orifice conditions at time,  $t=8$  seconds**

<b>Model</b>	<b>Flow rate (lpm) at, <math>t = 8</math> seconds</b>	<b>Difference compared to healthy data</b>
Healthy	393	-
10% increase in orifice area	397	4
25% increase in orifice area	490	97

50% increase in orifice area	590	197
75% increase in orifice area	688	295
90% increase in orifice area	747	354

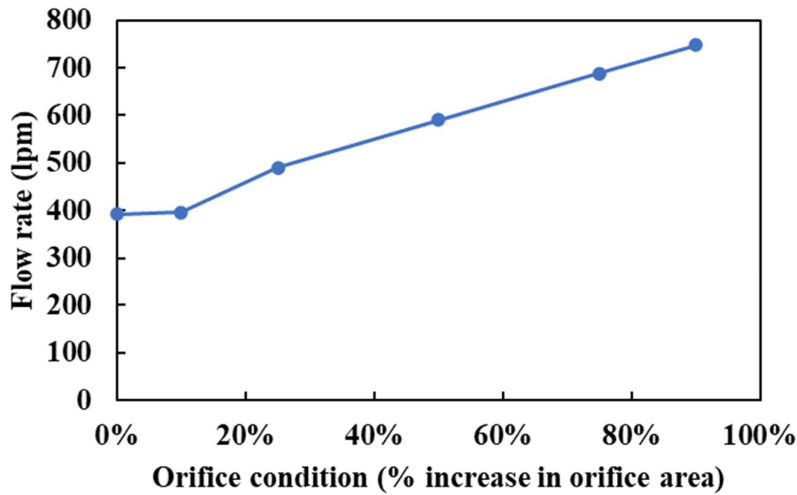


**Fig 4.5: Plot representing flow rate values under different orifice faults at time  $t=8$  sec.**

From table 4.2 and plot in fig 4.5, we can observe that the leakage at 10% fault is still less as compared to the leakage when the DC valve is run at 90% fault at time,  $t=8$  sec. But the difference with 10% fault at  $t=8$  sec is 4 lpm, whereas it was 0.9 lpm at  $t=2$  sec. It can be observed that the cumulative difference increases up to 50% fault and then slightly decreases, i.e., variation is more in beginning of the fault and then gradually reduces.

#### 4.4 Flow rate characteristics of DC valve with healthy orifice and faulty spool movement

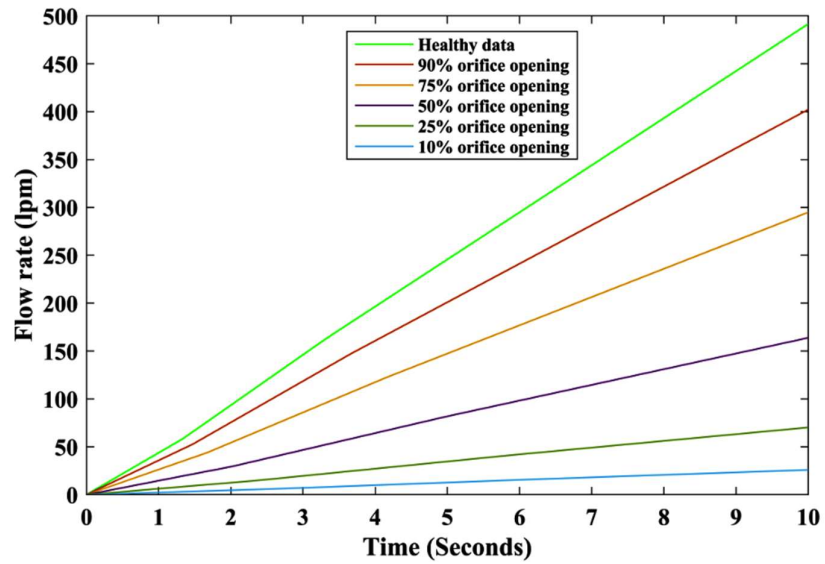


**Fig 4.6: Comparison of flow rate characteristics of DC valve under multiple spool faults**

The graph in figure (4.6) above shows a comparison of flow rate output from each model connected in a combination as shown in schematic figure (3.6). We can observe that with increase in the fault of spool movement the flow rate decreases as the orifice is not able to open completely.

As the orifice opening reduces the flow rate value reduces from the healthy case.

To understand the change in flow rate characteristics of each model, the below table shows the comparison of flow rate values at time,  $t = 2$  seconds, and  $t=8$  seconds.

Table 4.3: Flow rate values with different orifice conditions due to faulty spool movement at time, t=2 seconds

Model	Flow rate (lpm) at, t = 2 seconds	Difference compared to healthy data
Healthy	93.4	-
90% orifice opening	47.7	-45.7
75% orifice opening	35	-58.4
50% orifice opening	19.5	-73.9
25% orifice opening	8.36	-85.04
10% orifice opening	3.08	-90.32

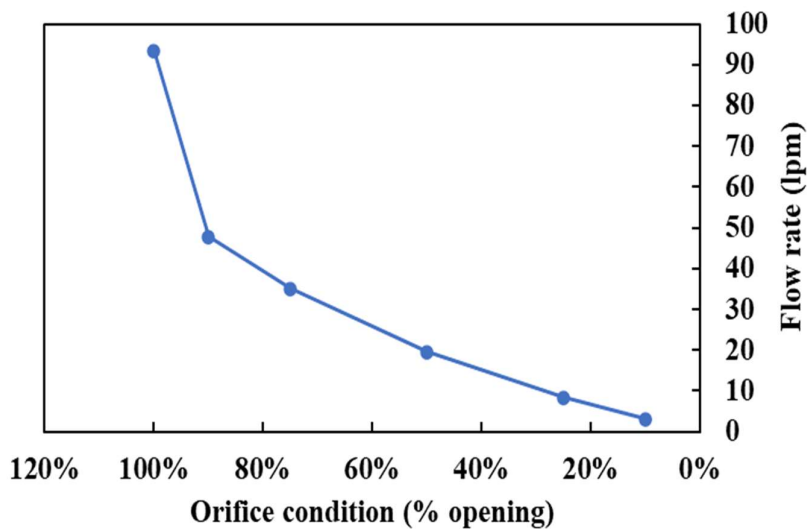


**Fig 4.7: Plot representing flow rate values under multiple spool faults at time t=2 sec.**

We observe that the flow rate value drastically decreases when the orifice opening is reduced by 10% due to faulty spool movement. The flow rate then keep on decreasing with increasing fault condition but the cumulative difference is less as compared to the fault in beginning.

Table 4.4: Flow rate values with different orifice conditions due to faulty spool movement at time, t=8 seconds

<b>Model</b>	<b>Flow rate (lpm) at, t = 8 sec</b>	<b>Difference compared to healthy data</b>
Healthy	393	-
90% orifice opening	214	-182
75% orifice opening	157	-236
50% orifice opening	87.3	-305.7
25% orifice opening	37.2	-355.8
10% orifice opening	13.6	-379.4

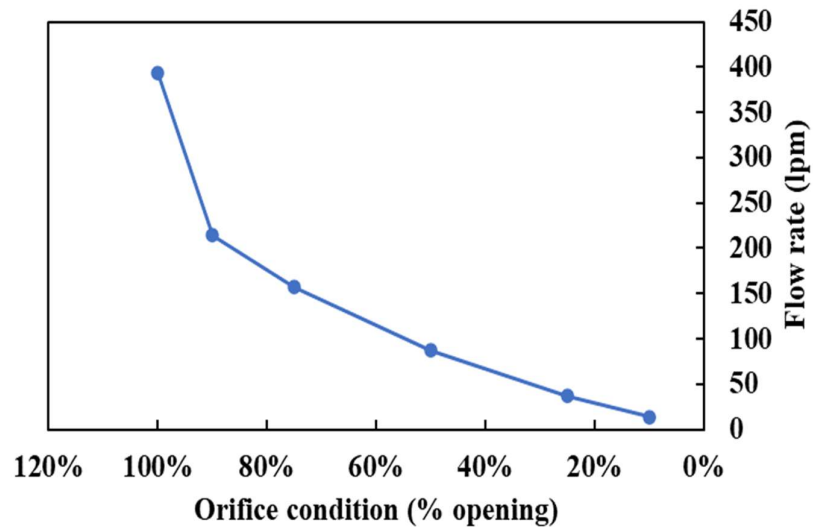


**Fig 4.8: Plot representing flow rate values under multiple spool faults at time t=8 sec.**

We observe that the flow rate value drastically decreases when the orifice opening is reduced by 10% due to faulty spool movement. The flow rate then keep on decreasing with increasing fault condition but the cumulative difference is less as compared to the fault in beginning.

We also observe that as time increases from 2 sec to 8 sec, the variation is more evident.

## 4.5 Flow rate characteristics with multiple faulty orifice and faulty spool movement

### Case 1: 10% orifice fault

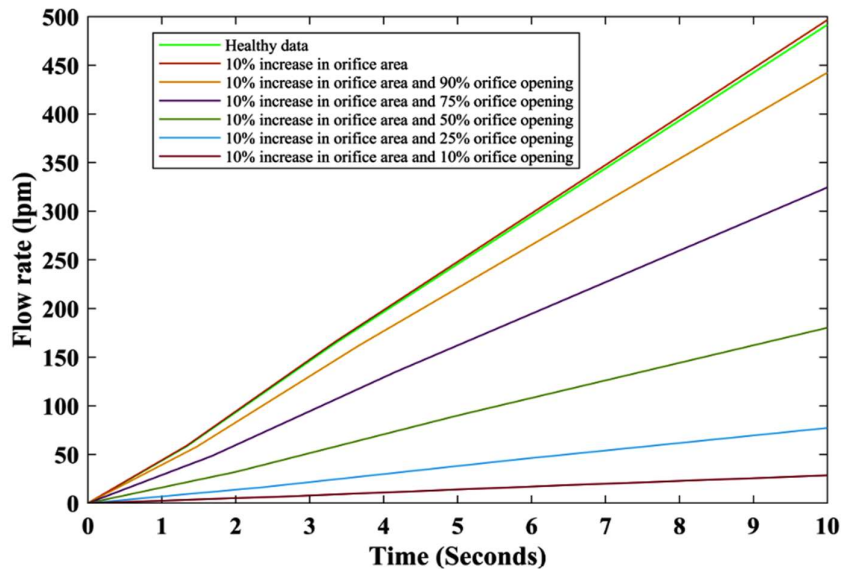


**Fig 4.9: Comparison of flow rate characteristics of DC valve under 10% increase in orifice area and multiple spool faults**

The graph in figure (4.9) above shows a comparison of flow rate output from each model connected in a combination as shown in schematic figure (3.7). We can observe that initially the flow rate increases slightly as the orifice area increase by 10% due to wear. But as we integrate the spool movement fault, we observe a decrement in flow rate from healthy condition.

To understand the change in flow rate characteristics of each model, the below table shows the comparison of flow rate values at time,  $t = 2$  seconds, and  $t=8$  seconds.

Table 4.5: Flow rate values with 10% orifice fault and faulty spool movement at time,  $t=2$  seconds

<b>Fault condition</b>	<b>Model</b>	<b>Flow rate (lpm) at, <math>t = 2</math> seconds</b>	<b>Difference compared to healthy data</b>
1	Healthy	93.4	-
2	10% increase in orifice area	94.3	0.9
3	10% increase in orifice area and 90% orifice opening	83	-10.4
4	10% increase in orifice area and 75% orifice opening	59.7	-33.7
5	10% increase in orifice area and 50% orifice opening	32.1	-61.3
6	10% increase in orifice area and 25% orifice opening	13.7	-79.7
7	10% increase in orifice area and 10% orifice opening	5.07	-88.33

We observe that flow rate tends to decrease with increasing spool fault. This decrement is more up to 50% fault and then the variation starts decreasing

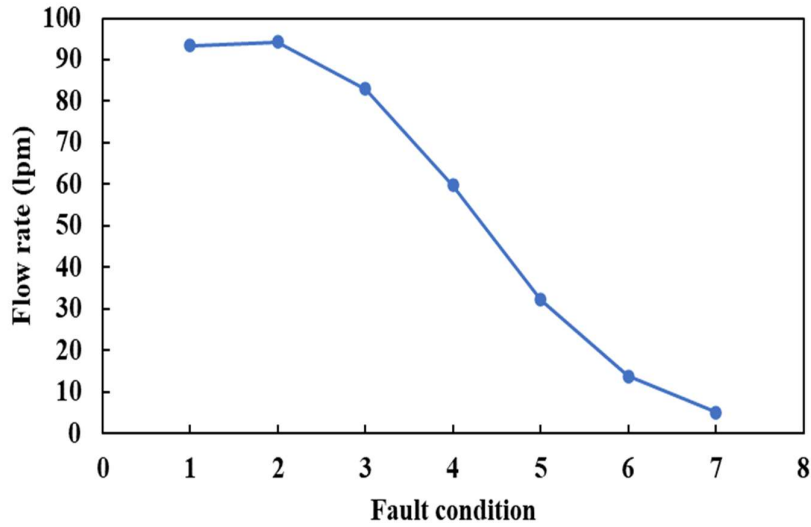


**Fig 4.10: Plot representing flow rate values under 10% orifice fault and faulty spool movement at time, t=2 seconds**

The variation in the decrement trend of flow rate due to the fault can be observed from the data points in graph. The variation increases up to 5<sup>th</sup> fault condition and is less in 6<sup>th</sup> and 7<sup>th</sup> condition.

**Table 4.6: Flow rate values with 10% orifice fault and faulty spool movement at time, t=8 seconds**

<b>Fault condition</b>	<b>Model</b>	<b>Flow rate (lpm) at, t = 8 seconds</b>	<b>Difference compared to healthy data</b>
1	Healthy	393	-
2	10% increase in orifice area	397	4
3	10% increase in orifice area and 90% orifice opening	354	-39
4	10% increase in orifice area and 75% orifice opening	259	-134
5	10% increase in orifice area and 50% orifice opening	144	-249

6	10% increase in orifice area and 25% orifice opening	61.8	331.2
7	10% increase in orifice area and 10% orifice opening	22.7	370.3

We observe that flow rate tends to decrease with increasing spool fault. This decrement is more up to 50% fault and then the variation starts decreasing.

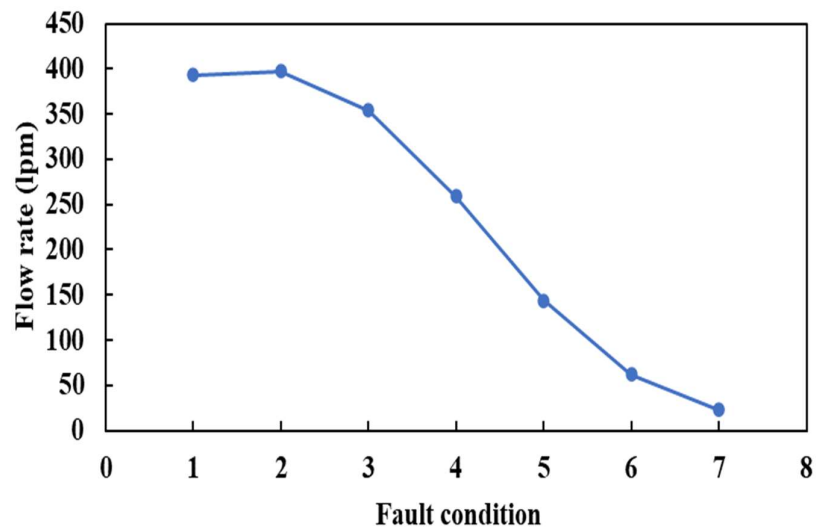


**Fig 4.11: Plot representing flow rate values under 10% orifice fault and faulty spool movement at time,  $t=8$  seconds.**

The variation in the decrement trend of flow rate due to the fault can be observed from the data points in graph. The variation increases up to 5<sup>th</sup> fault condition and is less in 6<sup>th</sup> and 7<sup>th</sup> condition.

We also observe that variation is more evident with increasing time, i.e., from  $t=2$  seconds to 8 seconds.

## Case 2: 25% orifice fault

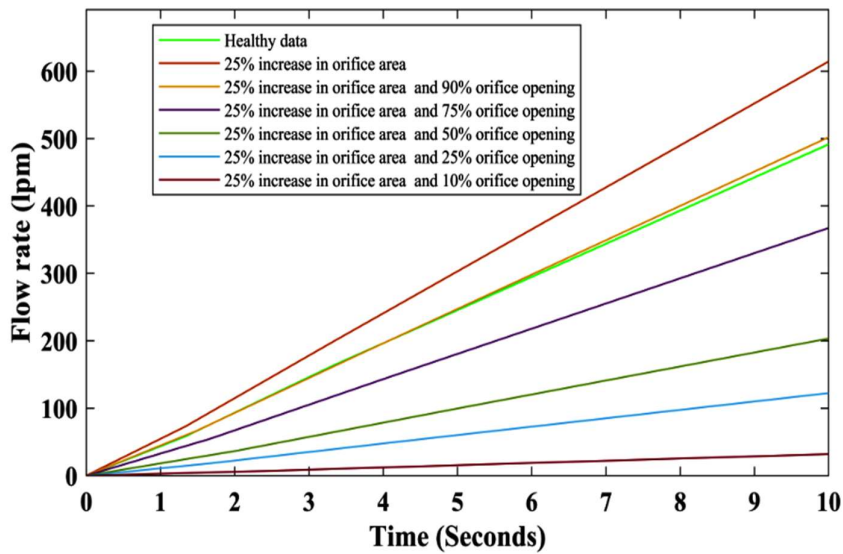


**Fig 4.12: Comparison of flow rate characteristics of DC valve under 25% increase in orifice area and multiple spool faults**

The graph in figure (4.12) above shows a comparison of flow rate output from each model according to the fault condition connected in a combination. We can observe that initially the flow rate increases as the orifice area increase by 25% due to wear. This initial increment is more than the increment in 10% case. But as we integrate the spool movement fault, we observe a decrement in flow rate from healthy condition.

We also observe that flow rate curve with 25% increase in orifice area and 90% orifice opening is slightly greater than the healthy case. Beyond this fault condition the flow rate trend decreases.

To understand the change in flow rate characteristics of each model, the below table shows the comparison of flow rate values at time,  $t = 2$  seconds, and  $t=8$  seconds.

Table 4.7: Flow rate values with 25% orifice fault and faulty spool movement at time,  $t=2$  seconds

<b>Fault condition</b>	<b>Model</b>	<b>Flow rate (lpm) at, <math>t = 2</math> sec</b>	<b>Difference compared to healthy data</b>
1	Healthy	93.4	-
2	25% increase in orifice area	115	21.6
3	25% increase in orifice area and 90% orifice opening	93.2	-0.2
4	25% increase in orifice area and 75% orifice opening	67.3	-26.1
5	25% increase in orifice area and 50% orifice opening	36.5	-56.9
6	25% increase in orifice area and 25% orifice opening	22.4	-71
7	25% increase in orifice area and 10% orifice opening	5.76	-87.64

We observe that flow rate tends to decrease with increasing spool fault. This decrement is more up to 50% fault and then the variation starts decreasing.

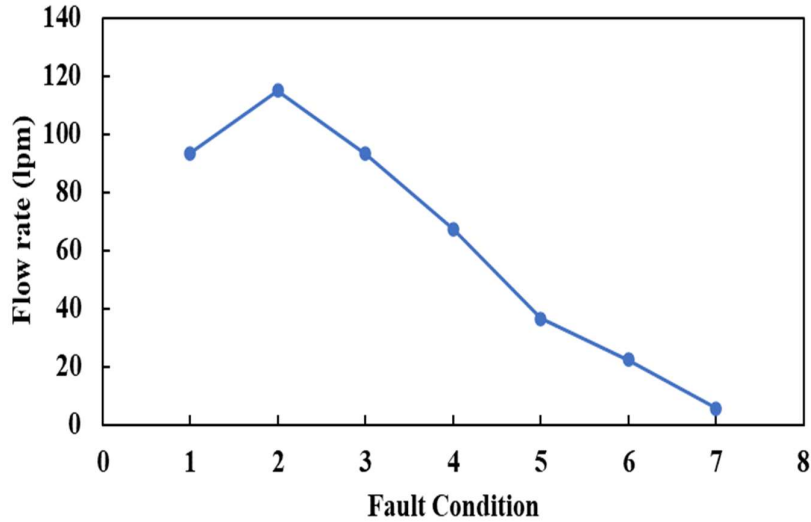


**Fig 4.13: Plot representing flow rate values under 25% orifice fault and faulty spool movement at time, t=2 seconds**

The variation in the decrement trend of flow rate due to the fault can be observed from the data points in graph. The increment in flow rate in 2<sup>nd</sup> fault condition is more visible than previous case with 10% fault. From the data points in the plot, we can also observe that variation of flow rate in 3<sup>rd</sup> fault condition and healthy case is very less.

**Table 4.8: Flow rate values with 25% orifice fault and faulty spool movement at time, t=8 seconds**

<b>Fault condition</b>	<b>Model</b>	<b>Flow rate (lpm) at, t = 8 sec</b>	<b>Difference compared to healthy data</b>
1	Healthy	393	-
2	25% increase in orifice area	490	97
3	25% increase in orifice area and 90% orifice opening	400	7
4	25% increase in orifice area and 75% orifice opening	293	-100

5	25% increase in orifice area and 50% orifice opening	162	-231
6	25% increase in orifice area and 25% orifice opening	97.6	-295.4
7	25% increase in orifice area and 10% orifice opening	25.4	-367.6

We observe that flow rate tends to decrease with increasing spool fault. This decrement is more up to 50% fault and then the variation starts decreasing.

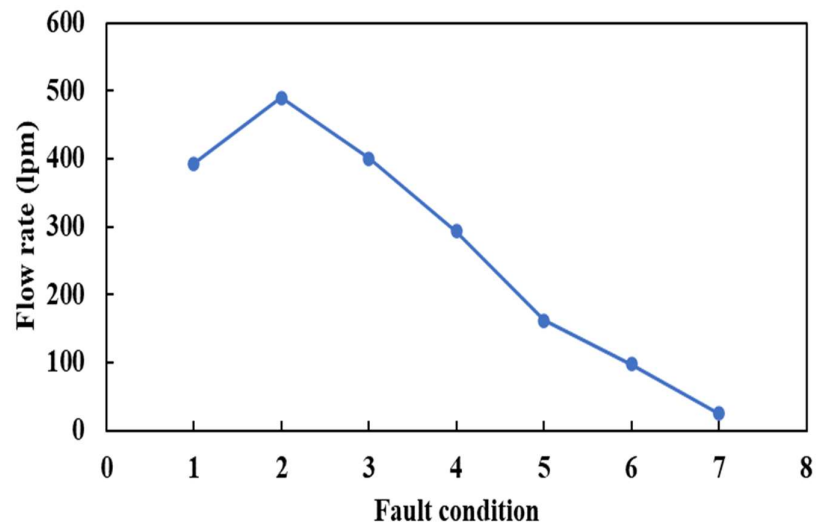


**Fig 4.14: Plot representing flow rate values under 25% orifice fault and faulty spool movement at time, t=8 seconds**

The variation in the decrement trend of flow rate due to the fault can be observed from the data points in graph. The variation increases up to 5<sup>th</sup> fault condition and is less in 6<sup>th</sup> and 7<sup>th</sup> condition.

We also observe that variation is more evident with increasing time, i.e., from t=2 seconds to 8 seconds.

### Case 3: 50% orifice fault

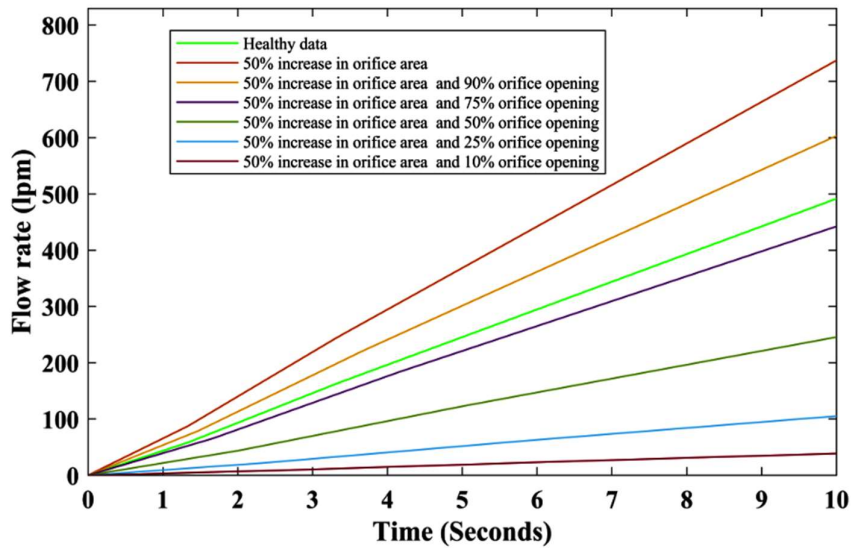


**Fig 4.15: Comparison of flow rate characteristics of DC valve under 50% increase in orifice area and multiple spool faults**

The graph in figure (4.15) above shows a comparison of flow rate output from each model according to the fault condition connected in a combination. We can observe that initially the flow rate increases as the orifice area increase by 50% due to wear. This initial increment is more than the previous two cases. But as we integrate the spool movement fault, we observe a decrement in flow rate.

We also observe that flow rate curve with 25% increase in orifice area and 90% orifice opening is greater than the healthy case. Beyond this fault condition, the flow rate trend decreases.

To understand the change in flow rate characteristics of each model, the below table shows the comparison of flow rate values at time,  $t = 2$  seconds, and  $t=8$  seconds.

Table 4.9: Flow rate values with 50% orifice fault and faulty spool movement at time,  $t=2$  seconds

<b>Fault condition</b>	<b>Model</b>	<b>Flow rate (lpm) at, <math>t = 2</math> sec</b>	<b>Difference compared to healthy data</b>
1	Healthy	93.4	-
2	50% increase in orifice area	140	46.6
3	50% increase in orifice area and 90% orifice opening	113	19.6
4	50% increase in orifice area and 75% orifice opening	81.4	-12
5	50% increase in orifice area and 50% orifice opening	43.8	-49.6
6	50% increase in orifice area and 25% orifice opening	18.8	-74.6
7	50% increase in orifice area and 10% orifice opening	6.91	-86.49

We observe the same decreasing trend in flow rate as in previous case. The variation is more as compared to the case with 25% fault. For example, the flow rate for fault condition 3 and 7 in this case is 113 lpm and 6.91 lpm respectively, whereas it was 93.2 lpm and 5.76 lpm for the previous case.

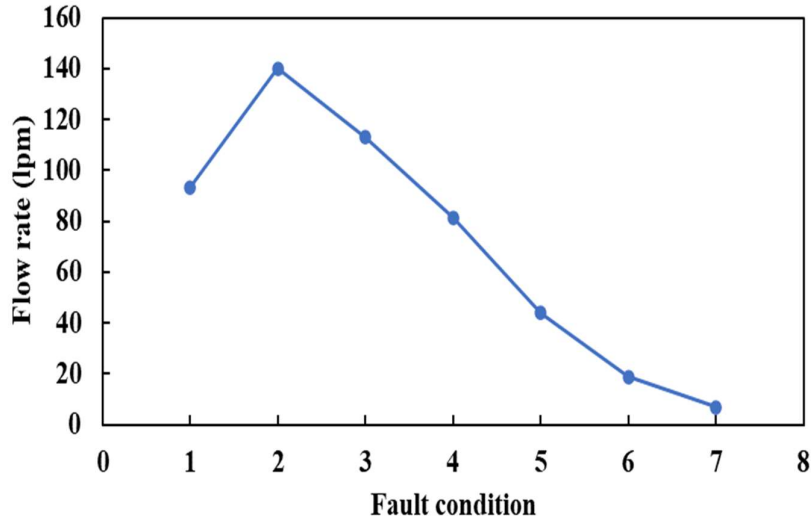


**Fig 4.16: Plot representing flow rate values under 50% orifice fault and faulty spool movement at time,  $t=2$  seconds**

The variation in the decrement trend of flow rate due to the fault can be observed from the data points in graph. The variation increases up to 5<sup>th</sup> fault condition and is less in 6<sup>th</sup> and 7<sup>th</sup> condition.

**Table 4.10: Flow rate values with 50% orifice fault and faulty spool movement at time,  $t=8$  seconds**

<b>Fault condition</b>	<b>Model</b>	<b>Flow rate (lpm) at, <math>t = 8</math> seconds</b>	<b>Difference compared to healthy data</b>
1	Healthy	393	-
2	50% increase in orifice area	590	197
3	50% increase in orifice area and 90% orifice opening	483	90

4	50% increase in orifice area and 75% orifice opening	354	-39
5	50% increase in orifice area and 50% orifice opening	197	-196
6	50% increase in orifice area and 25% orifice opening	84.2	-308.8
7	50% increase in orifice area and 10% orifice opening	31	-362

We observe that flow rate tends to decrease with increasing spool fault. This decrement is more up to 50% fault and then the variation starts decreasing.

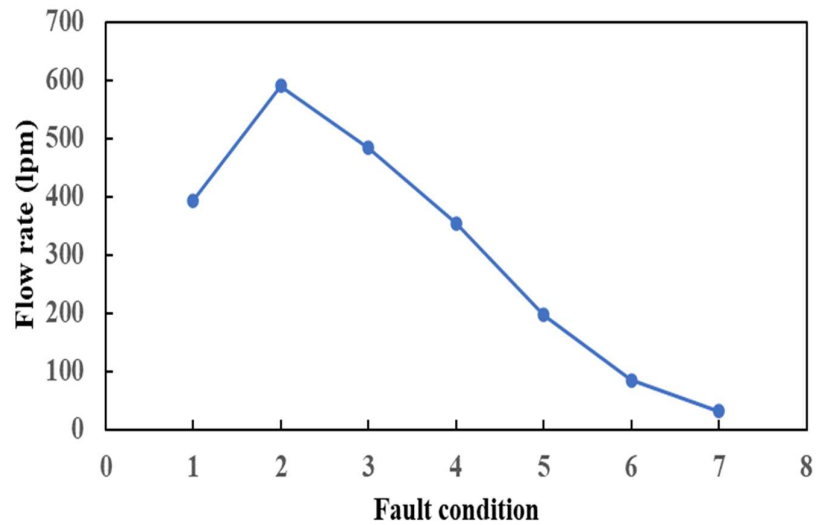


**Fig 4.17: Plot representing flow rate values under 50% orifice fault and faulty spool movement at time, t=8 seconds**

The variation in flow rate shows similar trend as it was at time t=2 seconds. But the difference in flow rate is more evident than it was at 2 seconds.

#### Case 4: 75% orifice fault

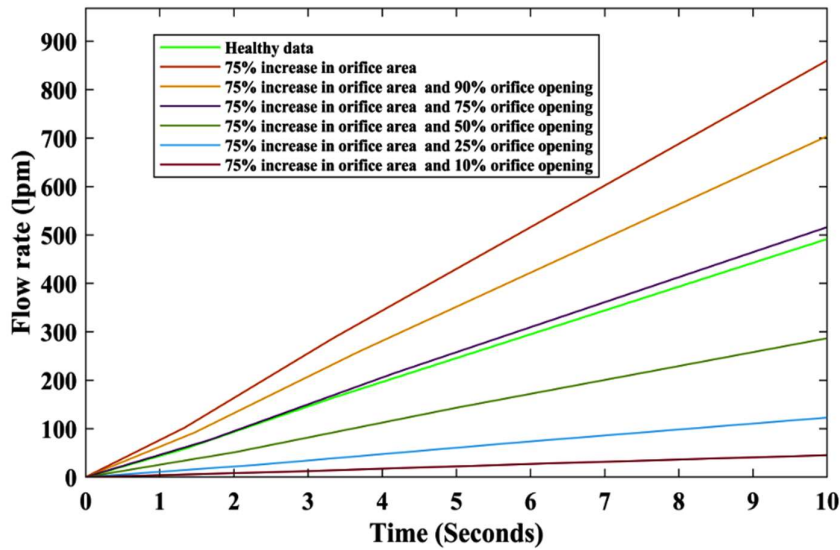


**Fig 4.18: Comparison of flow rate characteristics of DC valve under 75% increase in orifice area and multiple spool faults**

The graph in figure (4.18) above shows a comparison of flow rate output from each model according to the fault condition connected in a combination. We can observe that initially the flow rate increases as the orifice area increase by 75% due to wear. This initial increment is more than the previous three cases. But as we integrate the spool movement fault, we observe a decrement in flow rate.

We also observe that flow rate curve with 2<sup>nd</sup>, 3<sup>rd</sup> and 4<sup>th</sup> fault case is greater than the healthy case. Beyond this fault condition, the flow rate trend decreases.

To understand the change in flow rate characteristics of each model, the below table shows the comparison of flow rate values at time, t = 2 seconds, and t=8 seconds.

Table 4.11: Flow rate values with 75% orifice fault and faulty spool movement at time,  $t=2$  seconds

<b>Fault condition</b>	<b>Model</b>	<b>Flow rate (lpm) at, <math>t=2</math> sec</b>	<b>Difference compared to healthy data</b>
1	Healthy	93.4	-
2	75% increase in orifice area	163	69.6
3	75% increase in orifice area and 90% orifice opening	132	38.6
4	75% increase in orifice area and 75% orifice opening	94.9	1.5
5	75% increase in orifice area and 50% orifice opening	51.1	-42.3
6	75% increase in orifice area and 25% orifice opening	21.9	-71.5
7	75% increase in orifice area and 10% orifice opening	8.06	-85.34

We observe the same decreasing trend in flow rate as in previous case. The variation is more as compared to the case with 25% fault and 50% fault.

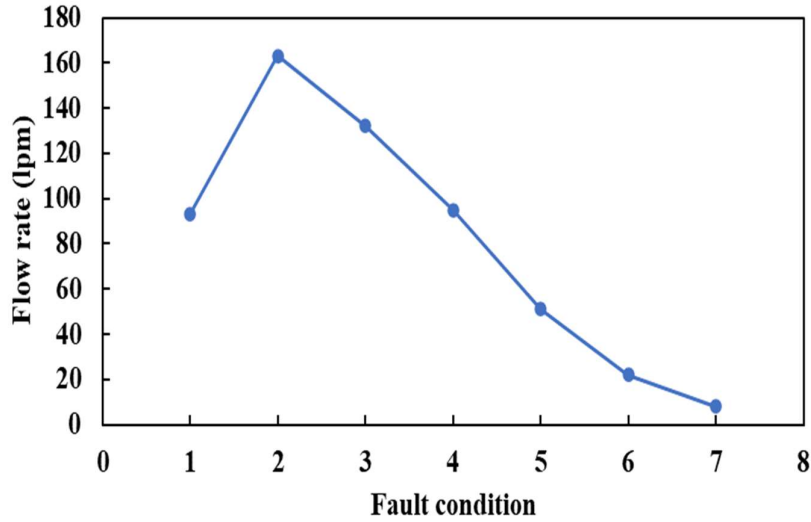


**Fig 4.19: Plot representing flow rate values under 75% orifice fault and faulty spool movement at time, t=2 seconds**

The variation in the decrement trend of flow rate due to the fault can be observed from the data points in graph. The variation increases up to 5<sup>th</sup> fault condition and is less in 6<sup>th</sup> and 7<sup>th</sup> condition.

**Table 4.12: Flow rate values with 75% orifice fault and faulty spool movement at time, t=8 seconds**

<b>Fault condition</b>	<b>Model</b>	<b>Flow rate (lpm) at, t = 8 seconds</b>	<b>Difference compared to healthy data</b>
1	Healthy	393	-
2	75% increase in orifice area	688	295
3	75% increase in orifice area and 90% orifice opening	563	170

4	75% increase in orifice area and 75% orifice opening	413	20
5	75% increase in orifice area and 50% orifice opening	229	-164
6	75% increase in orifice area and 25% orifice opening	98.2	-294.8
7	75% increase in orifice area and 10% orifice opening	36.2	-356.8

We observe that flow rate tends to decrease with increasing spool fault. This decrement is more up to 50% fault and then the variation starts decreasing.

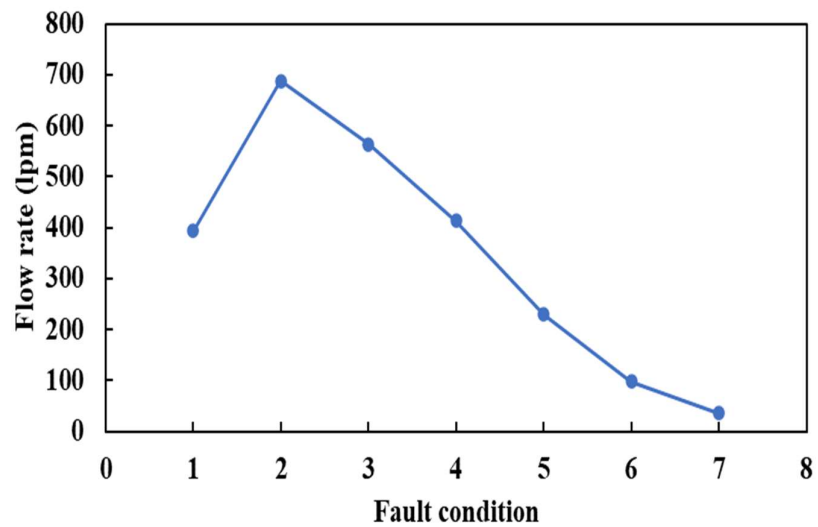


**Fig 4.20: Plot representing flow rate values under 75% orifice fault and faulty spool movement at time, t=8 seconds**

The variation in flow rate shows similar trend as it was at time t=2 seconds. But the difference in flow rate is more evident than it was at 2 seconds.

### Case 5: 90% orifice fault

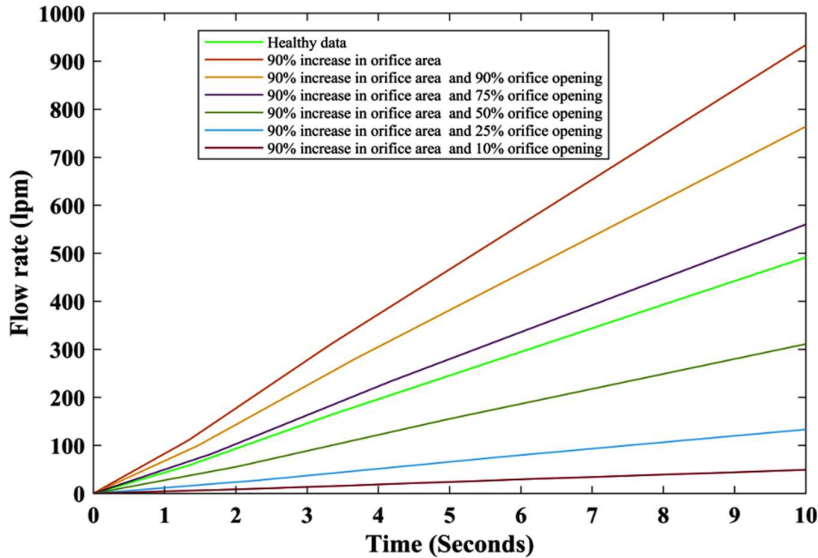


**Fig 4.21: Comparison of flow rate characteristics of DC valve under 90% increase in orifice area and multiple spool faults**

The graph in figure (4.21) above shows a comparison of flow rate output from each model according to the fault condition connected in a combination. We can observe that initially the flow rate increases as the orifice area increase by 90% due to wear. This initial increment is more than the previous four cases. But as we integrate the spool movement fault, we observe a decrement in flow rate.

We also observe that flow rate curve with 2<sup>nd</sup>, 3<sup>rd</sup> and 4<sup>th</sup> fault case is greater than the healthy case. Beyond this fault condition, the flow rate trend decreases.

To understand the change in flow rate characteristics of each model, the below table shows the comparison of flow rate values at time, t = 2 seconds, and t=8 seconds.

Table 4.13: Flow rate values with 90% orifice fault and faulty spool movement at time,  $t=2$  seconds

<b>Fault condition</b>	<b>Model</b>	<b>Flow rate (lpm) at, <math>t = 2</math> sec</b>	<b>Difference compared to healthy data</b>
1	Healthy	93.4	-
2	90% increase in orifice area	177	83.6
3	90% increase in orifice area and 90% orifice opening	143	49.6
4	90% increase in orifice area and 75% orifice opening	103	9.6
5	90% increase in orifice area and 50% orifice opening	55.5	-37.9
6	90% increase in orifice area and 25% orifice opening	23.8	-69.6
7	90% increase in orifice area and 10% orifice opening	8.75	84.65

We observe the same decreasing trend in flow rate as in previous case. The variation is more as compared to the case with 25% fault, 50% fault and 75% fault.

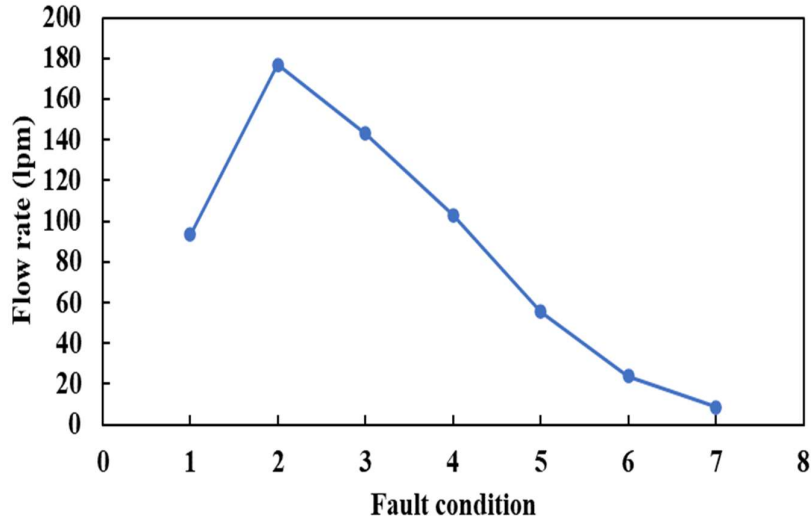


**Fig 4.22: Plot representing flow rate values under 90% orifice fault and faulty spool movement at time, t=2 seconds.**

The variation in the decrement trend of flow rate due to the fault can be observed from the data points in graph. The variation increases up to 5<sup>th</sup> fault condition and is less in 6<sup>th</sup> and 7<sup>th</sup> condition.

**Table 4.14: Flow rate values with 90% orifice fault and faulty spool movement at time, t=8 seconds**

<b>Fault condition</b>	<b>Model</b>	<b>Flow rate (lpm) at, t = 8 sec</b>	<b>Difference compared to healthy data</b>
1	Healthy	393	-
2	90% increase in orifice area	747	354
3	90% increase in orifice area and 90% orifice opening	611	218
4	90% increase in orifice area and 75% orifice opening	448	55
5	90% increase in orifice area and 50% orifice opening	249	-144

6	90% increase in orifice area and 25% orifice opening	107	-286
7	90% increase in orifice area and 10% orifice opening	39.3	-353.7

We observe that flow rate tends to decrease with increasing spool fault. This decrement is more up to 50% fault and then the variation starts decreasing. The same can be seen from the cumulative difference in table.

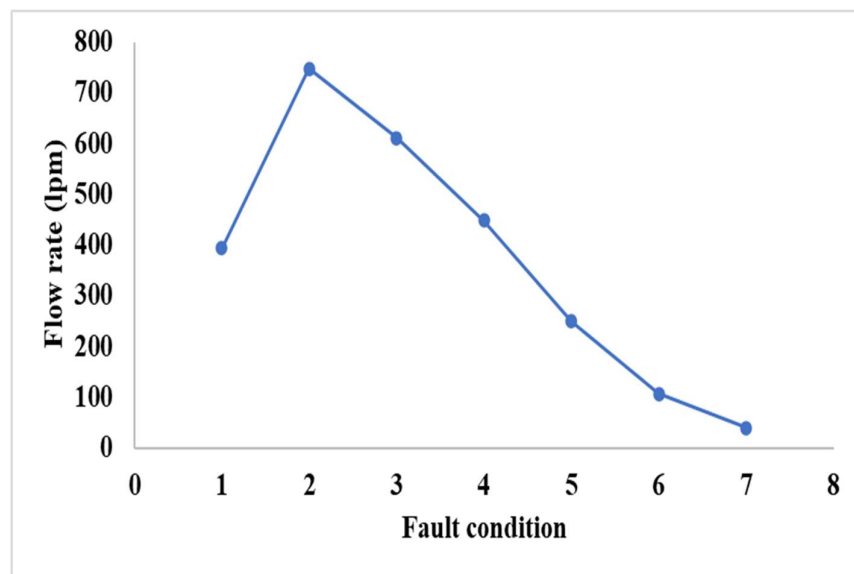


**Fig 4.23: Plot representing flow rate values under 90% orifice fault and faulty spool movement at time,  $t=8$  seconds.**

The variation in flow rate shows similar trend as it was at time  $t=2$  seconds. But the difference in flow rate is more evident than it was at 2 seconds.

## 4.6 Comparison of all five faulty cases

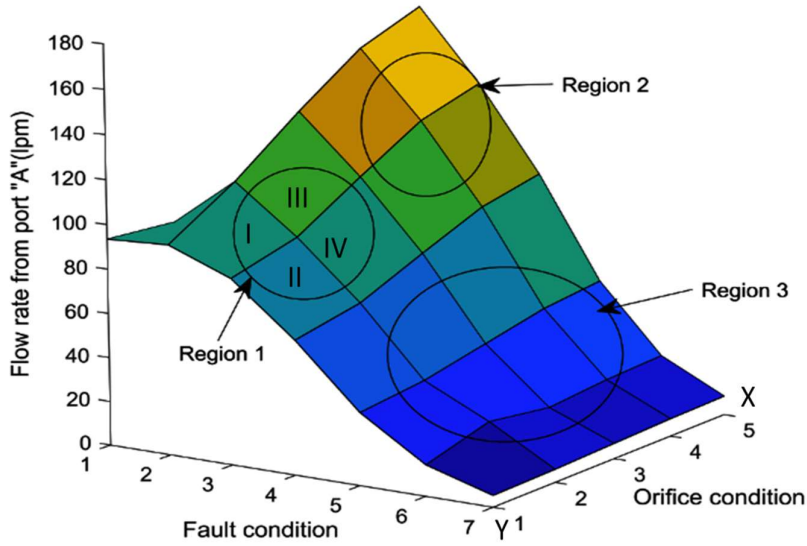


Fig 4.24: 3-D plot comparing all 5 cases at time,  $t=2$  seconds

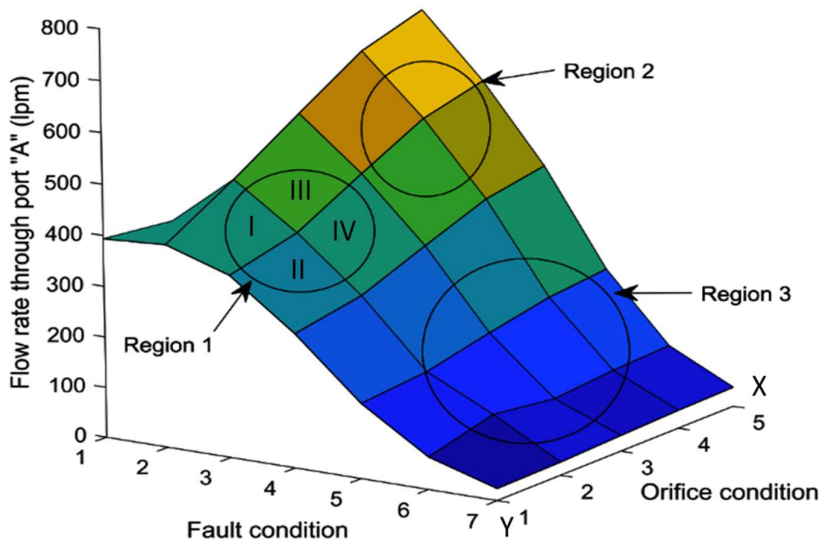


Fig 4.25: 3-D plot comparing all 5 cases at time,  $t=8$  seconds

Table 4.15: Table defining axis of the plots in fig 4.24 and 4.25

<b>X-axis</b>	<b>Orifice condition (% increase in orifice area)</b>	<b>Y-axis</b>	<b>Fault condition</b>
1	10	1	Healthy or No spool fault
2	25	2	Increase in orifice area same as the orifice condition of that curve
3	50	3	90% orifice opening
4	75	4	75% orifice opening
5	90	5	50% orifice opening
		6	25% orifice opening
		7	10% orifice opening

Table 4.16: Table defining region 1 of the plots in fig 4.24 and 4.25

Region 1	<p>I. 10% increase in orifice area and 90% orifice opening</p> <p>II. 10% increase in orifice area and 75% orifice opening</p> <p>III. 25% increase in orifice area and 90% orifice opening</p> <p>IV. 25% increase in orifice area and 75% orifice opening</p>
----------	---

- We may observe from the combined results in figures 4.24 and 4.25 that DC valves can work with defects that have flow rate values near to the healthy case, i.e., in region 1. Extreme fault instances, such as area 2 and 3, are not recommended for operation as the variation is very large.

- From both the 3-D plots we can infer that flow rate value increases with wear in orifice and then starts to decline with fault in the spool movement.
- At fault condition 2 of the plot, we can observe the increasing flow rate as the orifice condition deteriorates. It is min at 1<sup>st</sup> orifice condition, i.e., 10% increase in orifice and maximum at extreme orifice condition of 90% increase in orifice area.
- The decline in the flow rate also differs with each fault condition. The difference is higher mostly till 5<sup>th</sup> fault condition and then reduces slightly.

## **Chapter 5**

### **Conclusion and future scope**

#### **5.1 Conclusion**

The focus and aim of the research work were to understand and compare the flow rate output from directional control valves under different fault conditions. The attempts in this regard have been proposed and explained throughout the thesis.

A MATLAB-SIMULINK based model study was carried out to understand the parameters and working of 4/3-way DC valve. A base model for DC valve was designed in SIMULINK with healthy parameters and its flow rate was analyzed and compared with the referral articles. To carry forward the study for fault conditions, the same model was used with modified parameters according to the fault case. These individual fault case models were then combined to observe the flow rate of different conditions together.

The results of the thorough investigation reveal that the above-mentioned method can be used to proficiently demonstrate the variation of flow rate of directional control valve. It also explains the trend of flow rate outputs under multiple leakage conditions, incomplete opening of orifice due to faulty spool movement and a combination of both. The comparison plots in the model output shows the variation of faulty cases with respect to the healthy case. To better understand these comparisons, the difference in the flow rate has been studied at 2 seconds and 8 seconds and shown graphically in the result section.

For the first fault case, where comparison of flow rates under multiple orifice faults has been studied, the difference from healthy case output shows an increasing trend with increasing fault at the orifice. The difference is negligible up to 10% fault but increases afterwards.

In the second case, where comparison of flow rates under healthy orifice and faulty spool movement has been studied, the flow rate output shows a decreasing trend with respect to the healthy case.

In third case, where multiple orifice fault and faulty spool movement condition has been studied in a combination, the flow rate output increases in the beginning when we consider fault just at the orifice, but as we start considering the fault in the spool movement, we observe a decreasing trend.

From all the results combined in figure 4.24 and 4.25 we can propose that DC valve can operate with faults having flow rate values close to the healthy case, i.e., in region 1. Whereas it is not advisable to operate in extreme fault cases, i.e., region 2 and region 3.

## **5.2 Future scope**

Even though many areas of this research work have been covered, there are numerous study gaps that could be included as future scope of this research activity.

- i. The simulation study can be carried forward by considering faults at multiple ports simultaneously. To attain more real-life condition, we can consider different wear at different orifices to account the variation in flow rate entering and exiting the directional control valves.
- ii. A combined study of leakage from orifice and leakage between spool and casing of DC valve can also be studied.
- iii. To understand the broader consequences of faults considered in present work, the effect of faulty DC valve on complete hydraulic system can be investigated. A SIMULINK model of complete hydraulic system with an actuator operated by DC valve can be used to observe the change in its pressure signals.

Also, various machine learning techniques like artificial neural network, support vector machine, decision tree, etc. can be implemented to detect the faults in DC valve.

## References:

- [1] N. D. Manring and R. C. Fales, “Hydraulic Control Systems, 2nd Edition,” 2020.
- [2] R. K. Mobley, “Hydraulic Fundamentals,” *Plant Engineer’s Handbook*, pp. 639–686, Jan. 2001, doi: 10.1016/B978-075067328-0/50042-2.
- [3] J. Shi *et al.*, “Fault diagnosis in a hydraulic directional valve using a two-stage multi-sensor information fusion,” *Measurement*, vol. 179, p. 109460, Jul. 2021, doi: 10.1016/J.MEASUREMENT.2021.109460.
- [4] Incorporated. Vickers, “Vickers industrial hydraulics manual,” 1993, Accessed: Apr. 25, 2022. [Online]. Available: [https://books.google.com/books/about/Vickers\\_Industrial\\_Hydraulics\\_Manual.html?id=wn4bAQAAAJ](https://books.google.com/books/about/Vickers_Industrial_Hydraulics_Manual.html?id=wn4bAQAAAJ)
- [5] N. S. Ranawat, P. K. Kankar, and A. Miglani, “Fault diagnosis in centrifugal pump using support vector machine and artificial neural network,” *Journal of Engineering Research*, vol. 9, pp. 99–111, Aug. 2021, doi: 10.36909/JER.EMSME.13881.
- [6] H. Theissen and H. Murrenhoff, “Hydraulic Systems, Basics,” in *Encyclopedia of Lubricants and Lubrication*, Berlin, Heidelberg: Springer Berlin Heidelberg, 2014, pp. 914–936. doi: 10.1007/978-3-642-22647-2\_149.
- [7] J. Prakash, P. K. Kankar, and A. Miglani, “Monitoring the Degradation in the Switching Behavior of a Hydraulic Valve Using Recurrence Quantification Analysis and Fractal Dimensions,” *Journal of Computing and Information Science in Engineering*, vol. 21, no. 6, Dec. 2021, doi: 10.1115/1.4050821/1106897.
- [8] P. Garimella and bin Yao, “Model based fault detection of an electro-hydraulic cylinder,” in *Proceedings of the 2005, American Control Conference, 2005.*, pp. 484–489. doi: 10.1109/ACC.2005.1469982.
- [9] J. Prakash and P. K. Kankar, “Determining the Working Behaviour of Hydraulic System Using Support Vector Machine,” *Lecture Notes in Mechanical Engineering*, pp. 781–791, 2021, doi: 10.1007/978-981-15-8025-3\_74.
- [10] J. C. Fitch, “Systems and Methods for Real-Time Condition Monitoring of Mechanical Machinery,” 1986. [Online]. Available: <https://about.jstor.org/terms>

- [11] M. S. R. Jadhav, M. Y. P. Ballal, M. A. R. Mane, and A. Professor, "Design of Hydraulic System-A Review." [Online]. Available: [www.ijtrd.com](http://www.ijtrd.com)
- [12] J. Prakash and P. K. Kankar, "Health prediction of hydraulic cooling circuit using deep neural network with ensemble feature ranking technique," *Measurement: Journal of the International Measurement Confederation*, vol. 151, Feb. 2020, doi: 10.1016/J.MEASUREMENT.2019.107225.
- [13] M. Khoshzaban-Zavarehi, "On-line condition monitoring and fault diagnosis in hydraulic system components using parameter estimation and pattern classification," 1997, doi: 10.14288/1.0080942.
- [14] "Handbook of Condition Monitoring," 1998, doi: 10.1007/978-94-011-4924-2.
- [15] P. A. Hogan, C. R. Burrows, and K. A. Edge, "Development of a knowledge based system for the diagnosis of faults in hydraulic circuits.," 1990.
- [16] B. Freyermuth, "An approach to model based fault diagnosis of industrial robots," in *Proceedings - IEEE International Conference on Robotics and Automation*, 1991, vol. 2, pp. 1350–1356. doi: 10.1109/robot.1991.131801.
- [17] John. Watton, *Condition monitoring and fault diagnosis in fluid power systems*. Chichester: Ellis Horwood, 1992.
- [18] D. R. Bull, D. R. Bull, C. R. Burrows, and K. A. Edge, "A Computational Tool for Failure Modes and Effects Analysis of Hydraulic Systems", Accessed: May 02, 2022. [Online]. Available: <http://citeseerx.ist.psu.edu/viewdoc/summary?doi=10.1.1.57.41>
- [19] N. Helwig, E. Pignanelli, and A. Schutze, "Condition monitoring of a complex hydraulic system using multivariate statistics," *Conference Record - IEEE Instrumentation and Measurement Technology Conference*, vol. 2015-July, pp. 210–215, Jul. 2015, doi: 10.1109/I2MTC.2015.7151267.
- [20] S. M. A. A. Choudhury, S. L. Shah, and N. F. Thornhill, "Different Types of Faults in Control Valves," *Advances in Industrial Control*, no. 9783540792239, pp. 137–141, 2008, doi: 10.1007/978-3-540-79224-6\_10.
- [21] S. K. Venkata and S. Rao, "Fault Detection of a Flow Control Valve Using Vibration Analysis and Support Vector Machine," *Electronics 2019, Vol. 8, Page 1062*, vol. 8, no. 10, p. 1062, Sep. 2019, doi: 10.3390/ELECTRONICS8101062.

- [22] N. S. Ranawat and B. P. Nandwana, "Study of the Effect of Leak Location in Water Pipeline Using CFD," *Lecture Notes in Mechanical Engineering*, pp. 173–181, 2021, doi: 10.1007/978-981-15-8704-7\_21.
- [23] "Study of the Effect of Leak Size on Flow Characteristics using Computational Fluid Dynamics | Solid State Technology." <http://www.solidstatetechnology.us/index.php/JSST/article/view/6854> (accessed May 31, 2022).
- [24] J. Prakash, P. K. Kankar, and A. Miglani, "Internal Leakage Detection in a Hydraulic Pump using Exhaustive Feature Selection and Ensemble Learning," *2021 International Conference on Maintenance and Intelligent Asset Management, ICMIAM 2021*, 2021, doi: 10.1109/ICMIAM54662.2021.9715216.
- [25] V. Tchkalov and S. Miller, "Parameterization of Directional and Proportional Valves in SimHydraulics", Accessed: May 02, 2022. [Online]. Available: <http://www.mathworks.com/matlabcentral/fileexchange/27260>.
- [26] "Four-port three-position directional control valve - MATLAB - MathWorks India." <https://in.mathworks.com/help/physmod/hydro/ref/4waydirectionalvalve.html> (accessed May 02, 2022).
- [27] V. Mishra<sup>1</sup> and S. Chandel<sup>2</sup>, "Modeling & parameterization of Directional Control Valves using Matlab-Simulink/Sim Hydraulics", Accessed: May 02, 2022. [Online]. Available: [www.ijetsr.com](http://www.ijetsr.com)